

# UNCLASSIFIED

AD NUMBER
AD886984
NEW LIMITATION CHANGE
TO Approved for public release, distribution unlimited
FROM Distribution authorized to U.S. Gov't. agencies and their contractors; Critical Technology; JUN 1971. Other requests shall be referred to Air Force Materials Lab., Wright Patterson AFB, OH 45433.
AUTHORITY
AFML ltr, 29 Mar 1972

THIS PAGE IS UNCLASSIFIED

AFML-TR-70-54

PART II

AD886984

2

## CERAMIC MATRIX COMPOSITES AS ARMOR MATERIALS

D. RAY JOHNSON

P. E. D. MORGAN

THE FRANKLIN INSTITUTE RESEARCH LABORATORIES

TECHNICAL REPORT AFML-TR-70-54, PART II

JUNE 1971

DDC  
RECEIVED  
AUG 27 1971  
D

This document is subject to special export controls and each transmittal to foreign governments or foreign nationals may be made only with prior approval of the Air Force Materials Laboratory (LLM), Wright-Patterson Air Force Base, Ohio 45433.

AIR FORCE MATERIALS LABORATORY  
AIR FORCE SYSTEMS COMMAND  
WRIGHT-PATTERSON AIR FORCE BASE, OHIO

65

AD No. \_\_\_\_\_  
DDC FILE COPY

# NOTICE

When Government drawings, specifications, or other data are used for any purpose other than in connection with a definitely related Government procurement operation, the United States Government thereby incurs no responsibility nor any obligation whatsoever; and the fact that the government may have formulated, furnished, or in any way supplied the said drawings, specifications, or other data, is not to be regarded by implication or otherwise as in any manner licensing the holder or any other person or corporation, or conveying any rights or permission to manufacture, use, or sell any patented invention that may in any way be related thereto.

ADDRESS	
UNIT	SECTION
NO.	SECTION
NO.	SECTION
DISTRIBUTION/AVAILABILITY CODES	
DIST.	AVAIL. RDC/EX SPECIAL
2	

Copies of this report should not be returned unless return is required by security considerations, contractual obligations, or notice on a specific document.

# **CERAMIC MATRIX COMPOSITES AS ARMOR MATERIALS**

*D. RAY JOHNSON*

*P. E. D. MORGAN*

This document is subject to special export controls and each transmittal to foreign governments or foreign nationals may be made only with prior approval of the Air Force Materials Laboratory (LLM), Wright-Patterson Air Force Base, Ohio 45433.


Distribution of this report is limited for the protection of technology relating to critical materials restricted by the Export Control Act.

## FOREWORD

This report was prepared by The Franklin Institute Research Laboratories under Contract No. F33615-69-C-1659. The contract was initiated under Project 7350, "Refractory Inorganic Nonmetallic Materials," Task 735001, "Refractory Inorganic Nonmetallic Materials: Non-Graphitic," and was administered under the direction of the Air Force Materials Laboratory (LLM), Wright-Patterson Air Force Base, Ohio with John R. Fenter acting as Project Engineer.

This report covers work conducted from 16 June 1969 to 15 January 1971, and was released by the authors in February 1971.

This report has been reviewed and is approved.



W. G. Ramke  
Chief, Ceramics and Graphite Br.  
Metals and Ceramics Division  
Air Force Materials Laboratory

UNCLASSIFIED

Security Classification

## DOCUMENT CONTROL DATA - R &amp; D

(Security classification of title, body of abstract and indexing annotation must be entered when the overall report is classified)

1. ORIGINATING ACTIVITY (Corporate author) The Franklin Institute Research Laboratories Benjamin Franklin Parkway Philadelphia, Pennsylvania 19103		2a. REPORT SECURITY CLASSIFICATION UNCLASSIFIED	
		2b. GROUP	
3. REPORT TITLE  CERAMIC MATRIX COMPOSITES AS ARMOR MATERIALS			
4. DESCRIPTIVE NOTES (Type of report and inclusive dates) Final Report 16 Jun 69 to 15 Jan 1971			
5. AUTHOR(S) (First name, middle initial, last name) D. Ray Johnson, Peter E. D. Morgan			
6. REPORT DATE June 1971	7a. TOTAL NO. OF PAGES 53	7b. NO. OF REFS 15	
8a. CONTRACT OR GRANT NO. F33615 - 69 - C - 1659	9a. ORIGINATOR'S REPORT NUMBER(S) F-C2575-01		
b. PROJECT NO. c. 7350 d. Task No. 735001	9b. OTHER REPORT NO(S) (Any other numbers that may be assigned this report) AFML-TR-70-54, Part II		
10. DISTRIBUTION STATEMENT This document is subject to special export controls and each transmittal to foreign governments or foreign nationals may be made only with prior approval of the Air Force Materials Laboratory (LLM), Wright-Patterson Air Force Base, Ohio 45433.			
11. SUPPLEMENTARY NOTES		12. SPONSORING MILITARY ACTIVITY Air Force Materials Laboratory Air Force Systems Command Wright-Patterson Air Force Base, Ohio	
13. ABSTRACT  Specimens of nichrome wire mesh reinforced, titania doped alumina and spinel have been fabricated by pressure calcining and ballistically tested. The samples were right circular cylinders, 4" diameter x 1/4-3/4" thick. Photographs of ballistically tested samples, illustrating the types of fracture incurred, are given. A six months feasibility study of these and other composites is reviewed. Microstructural examination shows no degradation of the wire reinforcement or the matrix materials during fabrication. Sapphire fibers and whiskers did not significantly enhance the properties of the spinel and alumina matrices; the sapphire whiskers were dissolved in the matrix materials during fabrication. (			

DD FORM 1473  
1 NOV 65

UNCLASSIFIED

Security Classification

UNCLASSIFIED

Security Classification

14	KEY WORDS	LINK A		LINK B		LINK C	
		ROLE	WT	ROLE	WT	ROLE	WT
	Pressure Calcintering						
	Reactive Hot Pressing						
	Aluminum Oxide						
	Magnesium Aluminate Spinel						
	Ceramic Armor						
	Ceramic Matrix Composites						
	Alumina-Nichrome						
	Alumina-Sapphire						
	Spinel-Nichrome						
	Spinel-Sapphire						

UNCLASSIFIED

Security Classification

## ABSTRACT

Specimens of nichrome wire mesh reinforced, titania doped alumina and spinel have been fabricated by pressure calcining and ballistically tested. The samples were right circular cylinders, 4" diameter x 1/4-3/4" thick. Photographs of ballistically tested samples, illustrating the types of fracture incurred, are given. A six months feasibility study of these and other composites is reviewed. Microstructural examination shows no degradation of the wire reinforcement or the matrix materials during fabrication. Sapphire fibers and whiskers did not significantly enhance the properties of the spinel and alumina matrices; the sapphire whiskers were dissolved in the matrix materials during fabrication.



## TABLE OF CONTENTS

<u>Section</u>	<u>Title</u>	<u>Page</u>
I	INTRODUCTION . . . . .	1
II	MATERIALS . . . . .	3
	1. Alumina . . . . .	3
	2. Spinel . . . . .	7
	3. Reinforcing Materials . . . . .	9
	a. Nichrome Mesh . . . . .	9
	b. Single Crystal Sapphire Fibers . . . . .	9
	c. Single Crystal Sapphire Whiskers . . . . .	9
III	PRESSURE CALCINTERING . . . . .	10
IV	MICROSTRUCTURE . . . . .	15
V	MECHANICAL PROPERTIES . . . . .	26
	1. Tensile Strength . . . . .	26
	2. Elastic Modulus . . . . .	33
	3. Microhardness . . . . .	35
	4. Fractography of Ballistically Tested Specimens . .	38
VI	CONCLUSIONS . . . . .	50
VII	RECOMMENDATIONS FOR FUTURE WORK. . . . .	51
	REFERENCES . . . . .	52

# LIST OF ILLUSTRATIONS

<u>Figure</u>	<u>Title</u>	<u>Page</u>
1	Comparative Microstructures of Pressure Calcintere Al <sub>2</sub> O <sub>3</sub> (a) Undoped, Replica Electron Micrograph, X10,000, (b) 4.76 m/o TiO <sub>2</sub> , Scanning Electron Micro- graph, X10,000 . . . . .	4
2	Thermogravimetric Analysis of Al(OH) <sub>3</sub> + 2.38 m/o Ti(OH) <sub>4</sub> . . . . .	6
3	Thermogravimetric Analysis of Coprecipitated Al(OH) <sub>3</sub> , Mg(OH) <sub>2</sub> , and Ti(OH) <sub>4</sub> . . . . .	8
4	Interior Assembly of Hot Press for Fabrication of 3/4" Diameter Specimens . . . . .	11
5	Densification Curves for Pressure Calcintere Alumina and Spinel . . . . .	12
6.	Interior Assembly of Hot Press for Fabrication of 4" Diameter Specimens. . . . .	13
7.	Scanning Electron Micrograph of Spinel-Nichrome Wire Interface. Arrows Indicate Line Scanned for X-Ray Fluorescence . . . . .	16
8.	Intensity of Characteristic X-Rays Versus Distance Across the Nichrome Wire-Spinel Matrix Interface, a) Ni K <sub>α</sub> , b) Cr K <sub>α</sub> . . . . .	17
9.	Scanning Electron Micrograph of Nichrome Wire Re- inforced Alumina Showing the Grain Structure (a) Immediately Adjacent to the Wire and b) Removed from the Wire. Fracture Surface, X1000 . . . . .	19
10.	Scanning Electron Micrograph of Exposed Wire in Fractured Alumina-Nichrome Composite. a) X100, b) X300. . . . .	20
11.	Macrograph of Pressure Calcintere Spinel Contain- ing 15% by Weight of 0.5μ Sapphire Whiskers. Fracture Surface, X5.7 . . . . .	21
12.	Scanning Electron Micrograph of Pressure Calcintere Spinel Containing 15% by Weight 0.5μ Sapphire Whis- kers. Arrows Indicate Line Scanned for X-Ray Fluorescence. X600 . . . . .	21

# LIST OF ILLUSTRATIONS (cont'd)

<u>Figure</u>	<u>Title</u>	<u>Page</u>
13	Scanning Electron Micrograph of Pressure Calcintered Spinel Containing 15% by Weight 0.5 $\mu$ Sapphire Whiskers. X3000 . . . . .	22
14	Intensity of Characteristic Al K $\alpha$ X-Rays Versus Distance Across the Sample Area Scanned. Refer to Figure 12 . . . . .	23
15	Fractograph of MgAl <sub>2</sub> O <sub>4</sub> - Sapphire Single Crystal Fiber Composite, Scanning Electron Microscope . . . . .	25
16	Sample Holder for Diametral Compression Strength Tests.	27
17	Load-Deformation Curves for Alumina Ceramic and Alumina-Nichrome Wire Mesh Composite . . . . .	30
18	Diametral Compression Test Samples of Alumina (Left) and Nichrome-Alumina Composite (Right) Showing Type of Fracture.	31
19	Ballistically Tested Alumina Specimen . . . . .	40
20	Ballistically Tested Alumina-Nichrome Wire Mesh Composite, 3 16x16/in Wire Meshes . . . . .	41
21	Ballistically Tested Alumina-Nichrome Wire Mesh Composite, 3 8x8/in Meshes . . . . .	41
22	Ballistically Tested Alumina-Nichrome Wire Mesh Composite, 2 8x8/in Meshes . . . . .	42
23	Ballistically Tested Alumina-Nichrome Wire Mesh Composite, 2 16x16/in Meshes . . . . .	42
24	Ballistically Tested Alumina-Nichrome Wire Mesh Composite, 4 16x16/in Meshes, 50 Caliber Shot . . . . .	43
25	Ballistically Tested Alumina-Nichrome Wire Mesh Composite, 4 16x16/in Meshes. 50 Caliber Shot . . . . .	43
26	Ballistically Tested Spinel Specimen . . . . .	44
27	Ballistically Tested Spinel Specimen . . . . .	44

# LIST OF ILLUSTRATIONS (cont'd)

<u>Figure</u>	<u>Title</u>	<u>Page</u>
28	Ballistically Tested Spinel-Nichrome Wire Mesh Composite, 3 16x16/in Meshes . . . . .	45
29	Ballistically Tested Spinel-Nichrome Wire Mesh Composite, 3 16x16/in Meshes . . . . .	45
30	Fracture Surface of Ballistically Tested Alumina-Nichrome Composite. . . . .	46
31	Backup Plate After Ballistic Test of Alumina-Nichrome Composite . . . . .	46
32	Side View of Ballistically Tested Alumina-Nichrome Composite . . . . .	47
33	Back (exit) Side of Ballistically Tested Alumina-Nichrome Composite . . . . .	48
34	Back (exit) Side of Ballistically Tested Alumina-Nichrome Composite . . . . .	48
35	Ballistically Tested Alumina-Nichrome Composite . . . . .	49
36	Ballistically Tested Alumina-Nichrome Composite . . . . .	49

## LIST OF TABLES

<u>Table</u>	<u>Title</u>	<u>Page</u>
1	Emission Spectrographic Chemical Analysis of Ti(OH) <sub>4</sub> Doped Al(OH) <sub>3</sub> and Resulting Pressure Cal- cintered TiO <sub>2</sub> Doped Al <sub>2</sub> O <sub>3</sub> Ceramic . . . . .	5
2	Emission Spectrographic Chemical Analysis of Ti(OH) <sub>4</sub> Doped Spinel Precursor and Resulting Pres- sure Calcintered TiO <sub>2</sub> Doped MgAl <sub>2</sub> O <sub>4</sub> Ceramic . . . . .	5
3	Diametral Compression Tensile Strengths . . . . .	28
4	Bend Strengths of Pressure Calcintered Alumina . . . . .	29
5	Diametral Compression Tensile Strengths of Sapphire Fiber Reinforced Spinel Specimens . . . . .	32
6	Elastic Modulus Data . . . . .	34
7	Microhardness Data . . . . .	36
8	Microhardness Data for a Nichrome Al <sub>2</sub> O <sub>3</sub> Composite . . . . .	37

## SECTION I

### INTRODUCTION

Extremely high hardness and compressive strength are required of materials for ballistic armor. Weight considerations often restrict ballistic materials to those with densities less than 4-5 g/cc. Dense, fine grained polycrystalline ceramics are obviously best suited to these requirements. However, ceramics are characteristically brittle at ambient temperature. Ceramic armor fractures catastrophically under the impact of a projectile and offers little or no "second hit" capability.

Metal wire reinforced ceramics would seem to offer the desirable ceramic properties as well as the toughness required for ballistic applications. Metal wires well bonded in a ceramic matrix should absorb significant amounts of ballistic impact energy by plastic deformation, holding the ceramic matrix together to prevent catastrophic failure. The higher coefficient of thermal expansion of most metals will leave a ceramic matrix in compression after cooling from forming temperatures. As ceramics normally fracture in tension, a residual compressive stress strengthens the material. This effect is already utilized in tempered glass and prestressed concrete.

Metal wire-ceramic composites are extremely difficult to fabricate by conventional ceramic forming methods. Sintering and hot pressing of the metal oxides, borides, and carbides of interest for ballistic armor application must normally be done at very high temperatures, typically 1500°C and higher; many metals would be molten, or, if the forming were done in air, most would oxidize and degrade badly. While some noble metal alloys are stable in air at elevated temperatures, they do not have the combination of high strength and toughness required for ballistic applications. Furthermore, many ceramic-metal systems are not chemically compatible at elevated temperatures. However, the use of low temperature forming methods and oxidation resistant metals would seem to be a solution to the problems inherent in the fabrication of metal wire-ceramic composites in air.

The approach taken in this investigation is to form composites of nichrome wire with alumina or magnesium aluminate at relatively low temperatures by pressure calcining.

Pressure calcining is the hot pressing of a decomposing precursor according to the reaction  $\text{solid A} \rightarrow \text{solid B} + \text{gas}$ . A significant amount of very low temperature densification occurs during the decomposition, as well as during any subsequent solid state phase changes. The method has been shown to be feasible for the low temperature formation of fully dense, fine grained ceramics.<sup>1-5</sup> Uniform, translucent composites of magnesia and stainless steel wire have been formed by this method.

Nichrome is stable in air to  $\sim 1100^{\circ}\text{C}$  and possesses good strength and ductility. Alumina and spinel are very hard and strong in compression, making them ideal candidates for ballistic armor. Nichrome has a much higher coefficient of thermal expansion than either of the two matrix materials. The differential thermal contraction between the metal and the matrix material during cooling from the forming temperature should leave the matrix with the desired residual compressive stress.

This research effort is divided into two distinct phases: Phase I, a feasibility study, and Phase II, an effort to optimize fabrication parameters and composite configurations for ballistic application.

The object of Phase I is to investigate the feasibility of forming continuous matrix composites of alumina and/or magnesium aluminate reinforced with nichrome wire mesh or single crystal sapphire whiskers or fibers, and to carry out limited preliminary characterization of the mechanical properties of these composites.

The object of Phase II is to scale up the fabrication from small ( $3/4$ " diameter) samples to 4" diameter right circular cylindrical samples, which are suitable for ballistic testing. Fabrication parameters and composite configurations are to be optimized whenever possible with respect to ballistic performance.

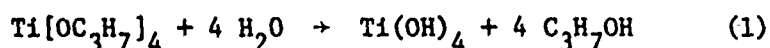
## SECTION II

### MATERIALS

Hydroxides have been found to be optimum precursors for the fabrication of dense, fine grained metal oxides by pressure calcinering. Hydrated alumina is readily available commercially and was used for forming alumina specimens. Suitable hydroxide precursors for spinel formation are not readily available; thus the magnesium aluminate precursor was produced by the authors. A very intimate mixture of reacting components is critically important for low temperature forming of spinel and other complex oxide ceramics. This intimate mixing is achieved by coprecipitation methods. The spinel precursor was coprecipitated from alkoxides and the alcohol-water by-products evaporated off. No washing or filtering was required. The alumina and spinel precursors were doped with  $\text{Ti}(\text{OH})_4$ , which decomposes to form  $\text{TiO}_2$  or other oxides containing  $\text{Ti}^{4+}$  during pressure calcinering. The  $\text{Ti}^{4+}$  acts as a densification aid and grain growth inhibitor. To insure intimate mixing of the  $\text{Ti}^{4+}$ , the  $\text{Ti}(\text{OH})_4$  was precipitated from the alkoxide along with the other components.

#### 1. Alumina

Titania doped alumina ceramics were formed from  $\text{Al}(\text{OH})_3^* + 2.38$  mole percent  $\text{Ti}(\text{OH})_4$ . During hot pressing the hydroxides decompose to form  $\text{Al}_2\text{O}_3 + 4.76$  mole percent  $\text{TiO}_2$ . The effect of Ti ions as a grain growth inhibitor in alumina is shown in Figure 1. The hydrated alumina was doped as follows: Titanium tetraisopropylate,\*\*  $\text{Ti}[\text{OC}_3\text{H}_7]_4$ , was added to a thick slurry of aluminum hydroxide in acetone and thoroughly blended in an electric food blender. The liquid titanium tetraisopropylate is soluble in acetone and, thus, becomes very intimately mixed into the slurry. The quantity of titanium tetraisopropylate added to the slurry was 8.72%, by weight, of the  $\text{Al}(\text{OH})_3$ . Distilled water was added dropwise to the blending slurry, 8 moles of water per mole of  $\text{Ti}[\text{OC}_3\text{H}_7]_4$ , according to the following reaction:



The quantity of water added is twice the amount required to insure completion of the hydrolysis reaction. The thick slurry was then transferred to a beaker and the acetone, alcohol, and water allowed to evaporate. Typical chemical analyses of the hydroxide precursor and a resultant pressure calcinered  $\text{Al}_2\text{O}_3$  sample are given in Table 1. A thermogravimetric analysis (TGA) of the powder is given in Figure 2. The TGA was performed\*\*\* at a constant heating rate of  $5^\circ\text{C}/\text{min}$  in an air atmosphere.

\* ALCOA C31 hydrated alumina, a product of the Aluminum Co. of America, Pittsburgh, Pa.

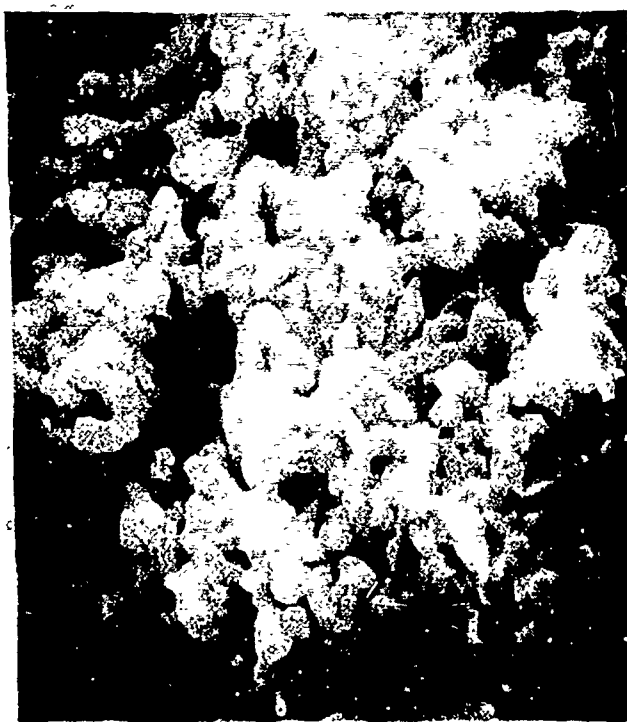
\*\* Tyzor tpt organic titanate, E. I. du Pont de Nemours & Co. (Inc.) Wilmington, Delaware.

\*\*\* Model 950 thermogravimetric analyzer, E. I. du Pont de Nemours & Co. (Inc.) Wilmington, Delaware.





(a)



(b)

Figure 1. Comparative Microstructures of Pressure Calcintered  $\text{Al}_2\text{O}_3$  (a) Undoped, Replica Electron Micrograph, X10,000, (b) 4.76 m/o  $\text{TiO}_2$ , Scanning Electron Micrograph, X10,000.

Table 1. EMISSION SPECTROGRAPHIC CHEMICAL ANALYSIS OF  $\text{Ti}(\text{OH})_4$   
DOPED  $\text{Al}(\text{OH})_3$  AND RESULTING PRESSURE CALCINTERED  $\text{TiO}_2$   
DOPED  $\text{Al}_2\text{O}_3$  CERAMIC

		CONCENTRATION, PPM								
		<u>Ag</u>	<u>B</u>	<u>Cu</u>	<u>Fe</u>	<u>Ga</u>	<u>Mg</u>	<u>Na</u>	<u>Si</u>	<u>Sn</u>
$\text{Ti}(\text{OH})_4$ Doped $\text{Al}(\text{OH})_3$		2	30	10	45	40	10	0.10%	30	N.D.
$\text{TiO}_2$ Doped $\text{Al}_2\text{O}_3$		N.D.	10	10	75	125	100	0.10%	50	50

Table 2. EMISSION SPECTROGRAPHIC CHEMICAL ANALYSIS OF  $\text{Ti}(\text{OH})_4$   
DOPED SPINEL PRECURSOR AND RESULTING PRESSURE CALCINTERED  
 $\text{TiO}_2$  DOPED  $\text{MgAl}_2\text{O}_4$  CERAMIC

		CONCENTRATION, PPM							
		<u>Ag</u>	<u>B</u>	<u>Cu</u>	<u>Fe</u>	<u>Ga</u>	<u>Ni</u>	<u>Si</u>	
$\text{Ti}(\text{OH})_4$ Doped Spinel Precursor		N.D.	30	35	75	60	N.D.	60	
$\text{TiO}_2$ Doped $\text{MgAl}_2\text{O}_4$		4	6	50	100	100	125	100	

Limits of detection for elements not detected (N.D.), PPM Ag(1), As(25), Ba(1), Be(1), Bi(1), Ca(1), Cb(100), Cd(10), Cr(1), Ge(5), Hg(50), In(1), Li(25), Mn(1), Mo(100), Na(25), Ni(10), P(100), Pb(1), Sb(10), Sr(25), Sn(10), Ta(250), Te(25), V(25), W(250), Zn(10), Zr(50)

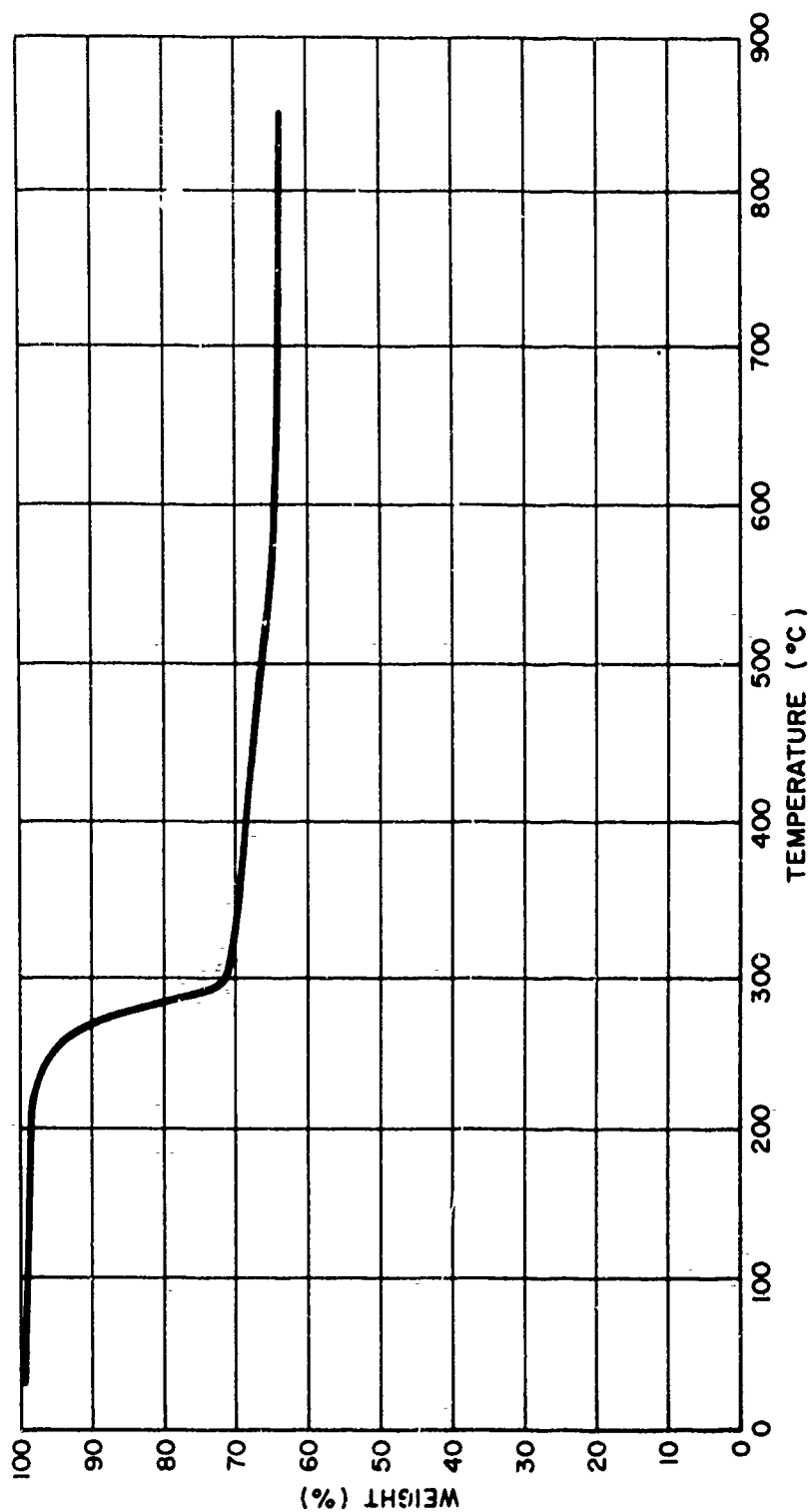
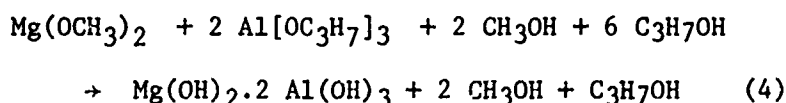
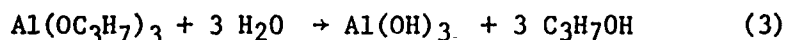
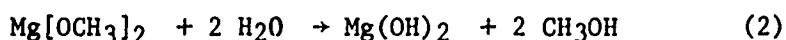
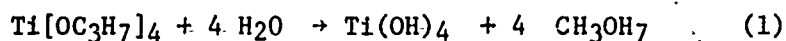


Figure 2. Thermogravimetric Analysis of  $\text{Al(OH)}_3 + 2.38 \text{ m/o Ti(OH)}_4$

## 2. Spinel

Titanium doped stoichiometric spinel was formed from  $\text{Mg}(\text{OH})_2$ ,  $2 \text{ Al}(\text{OH})_3$  + 2 mole %  $\text{Ti}(\text{OH})_4$ . The hydroxides decompose to form  $\text{MgAl}_2\text{O}_4$  + 2<sup>m/o</sup>  $\text{TiO}_2$  during hot pressing. The precursor was produced from aluminum isopropoxide,<sup>†</sup>  $\text{Al}[\text{OCH}(\text{CH}_3)_2]_3$ , magnesium methylate,  $\text{Mg}[\text{OCH}_3]_2$ , and titanium tetraisopropylate,  $\text{Ti}[\text{OC}_3\text{H}_7]_4$ . The procedure was as follows: The aluminum isopropoxide was dissolved in benzene in an electric food blender, after which a solution of magnesium methylate in methanol<sup>††</sup> and the titanium tetraisopropylate were blended in. Typically the quantities of aluminum isopropoxide and magnesium methylate required were 222.02 g aluminum isopropoxide per liter of magnesium methylate solution in methanol. To obtain 2<sup>m/o</sup>  $\text{TiO}_2$  in the  $\text{MgAl}_2\text{O}_4$ , 0.0139 g titanium tetraisopropylate per gram aluminum isopropoxide were required. Distilled water was then added dropwise to the blending solution, 10 moles of water per mole of  $\text{Mg}[\text{OCH}_3]_2$ , to hydrolyze the hydroxides as follows:



The resulting slurry was transferred to a beaker and the by-products were allowed to evaporate off. The amorphous powder may be a hydroxide glass; there is no evidence for the separate formation of  $\text{Mg}(\text{OH})_2$ ,  $\text{Al}(\text{OH})_3$  or complex mixed hydroxide crystal forms. To avoid excessive shrinkage during hot pressing, which can cause "crazing," the powder was heated to 350°C overnight. The prefired powder was still amorphous to X-rays. A typical differential thermal analysis is shown in Figure 3.

Typical chemical analyses for the spinel precursor powder and a spinel ceramic sample hot pressed from the powder are given in Table 2. Lattice parameter was measured for each batch of spinel produced. A small amount of the mixed hydroxide powder was calcined overnight at 1000 C and the X-ray diffraction pattern of the resultant spinel determined. X-ray diffraction was measured on a diffractometer\* using Ni filtered  $\text{Cu K}\alpha$  radiation. The diffraction patterns were determined over the range  $2\theta = 10^\circ$  to  $= 150^\circ$ . Cell size was calculated from each of the four highest angle peaks. These values were plotted against 20

<sup>†</sup> Practical grade aluminum isopropoxide, Chattanooga Chemicals, Chattanooga, Tenn.

<sup>††</sup> Magnesium methylate solution in methanol, Morton Chemicals, Chicago, Ill.

\* XRD-5 X-ray Diffraction Unit, Gen. Elec., Milwaukee, Wisconsin.

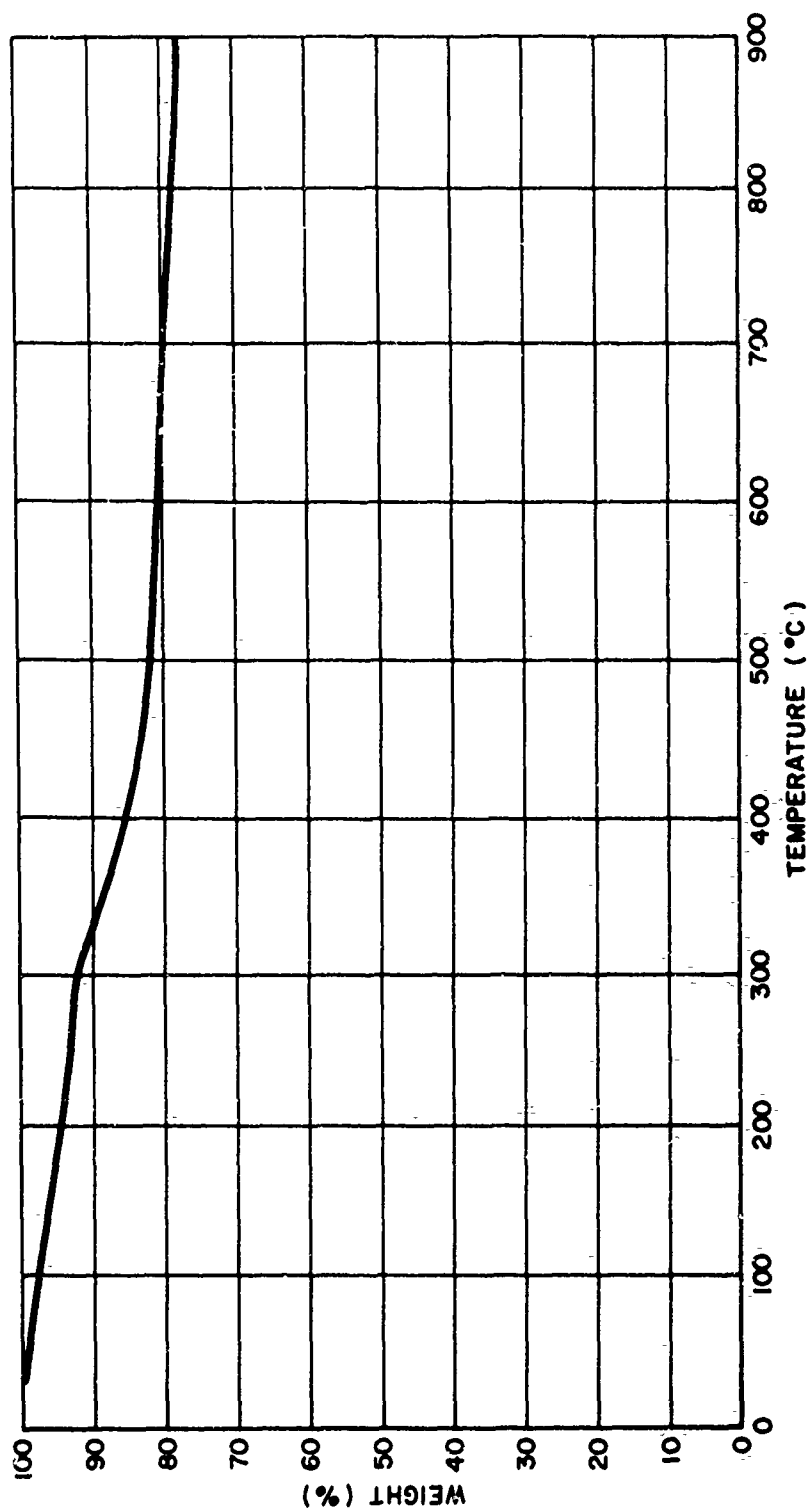


Figure 3. Thermogravimetric Analysis of Coprecipitated  $\text{Al(OH)}_3$ ,  $\text{Mg(OH)}_2$ , and  $\text{Ti(OH)}_4$

and extrapolated to  $2\theta = 180^\circ$  to determine the lattice parameter. The measured value was 8.082 Å in each case, in excellent agreement with values reported in the literature.<sup>7</sup> No T<sub>2</sub> second phase was apparent.

### 3. Reinforcing Materials

#### a. Nichrome Mesh

The nichrome mesh<sup>\*\*</sup> used in this investigation for nichrome-spinel and nichrome-alumina composites had the following nominal composition: 60 Ni-24 Fe-16 Cr. Typical properties of nichrome from the literature (see Reference 10) are as follows: density- 8.247 g/cc, Young's modulus-  $31 \times 10^6$  psi, melting point- 1425°C, tensile strength- 95,000 to 165,000 psi, Rockwell hardness- 85 to 105. Two different mesh sizes were used: 0.018" diameter wire woven into a 16x16 per inch mesh, and 0.025" diameter wire woven into an 8x8 per inch mesh. The wire was acquired in sheets from which 0.75" and 4.0" circular disks were cut.

#### b. Single Crystal Sapphire Fibers

A 10' continuous length of 0.010" diameter single crystal sapphire filament was acquired for use in this investigation. The manufacturer<sup>\*\*\*</sup> specifies an average tensile strength greater than 300,000 psi for this material. Short pieces, 1/4" to 3/4", of sapphire filament were hand broken from the continuous length for incorporation into small composite samples.

#### c. Single Crystal Sapphire Whiskers

The sapphire whiskers<sup>\*</sup> used for composites in this investigation were loose, bulk whiskers, 0.5μ in diameter. The whisker length was 2-20μ. The manufacturer specifies a tensile strength of 3 to 5 x  $10^6$  psi and a typical purity of 99.5% with minor AlN impurity and traces of Fe and Si. Previous investigators<sup>8</sup> found 0.5μ whiskers more favorable than other sizes for Al<sub>2</sub>O<sub>3</sub> composites.

<sup>\*\*</sup> Nichrome Wire Cloth, Newark Wire Cloth Co., Harrison, N. J.

<sup>\*\*\*</sup> Continuous single crystal sapphire filament, Tyco Laboratories, Cambridge, Mass.

<sup>\*</sup> Type 4-B single crystal sapphire whiskers, General Technologies Co., Reston, Va.

## SECTION III

### PRESSURE CALCINTERING

All hot pressing was done in porous (77% dense) spectroscopic grade graphite<sup>†</sup> dies. The gases generated during decomposition of the precursors diffuse through the porous graphite. The die assembly was heated in an electric resistance furnace; pressure was applied with a 50 ton platen press and a 10,000 psi hydraulic pump. A schematic diagram of the interior assembly of the hot press is shown in Figure 4.

A typical time-temperature program and resultant time-density profiles for alumina and spinel are shown in Figure 5. The pressure is applied at room temperature, maintained constant at 4000 psi to 1000°C, and then raised to 5000 psi from 1000 to 1350°C. These pressures represent the maximum safe values for our porous graphite dies. This has become our standard program for producing small (0.75" dia.), fully dense samples of spinel and alumina.

The scaling up of the process from fabrication of 3/4" to 4" diameter sample consisted of (1) modifying the hot press to accommodate the larger samples and accompanying higher mechanical and thermal loads; and (2) adjusting the hot pressing parameters to suitable values for the larger samples.

The new hot press for fabrication of large samples is similar to the previously described apparatus; a schematic diagram is shown in Figure 6. Pressure is applied with a 50 ton platen press and a 10,000 psi hydraulic pump, as before. The power supply for the furnace is a 10 KVA silicon control rectifier. Automatic temperature control is maintained with a curve-following programmer and a CAT controller. Temperature and sample length are recorded on a two-pen strip chart recorder. Hot pressing dies were constructed from porous (77% dense) spectroscopic grade graphite, as before.

The optimum hot pressing schedule for 4" diameter specimens of alumina and spinel ceramics and composites is as follows: A pressure of 2000 psi is applied at room temperature and heating is begun; at 1000°C the pressure is increased to 3000 psi, at 1200°C the pressure is increased to 4000 psi and remains at 4000 psi for the duration of the hot pressing.

---

<sup>†</sup> UF4S Graphite, Ultra Carbon Corp., Bay City, Michigan

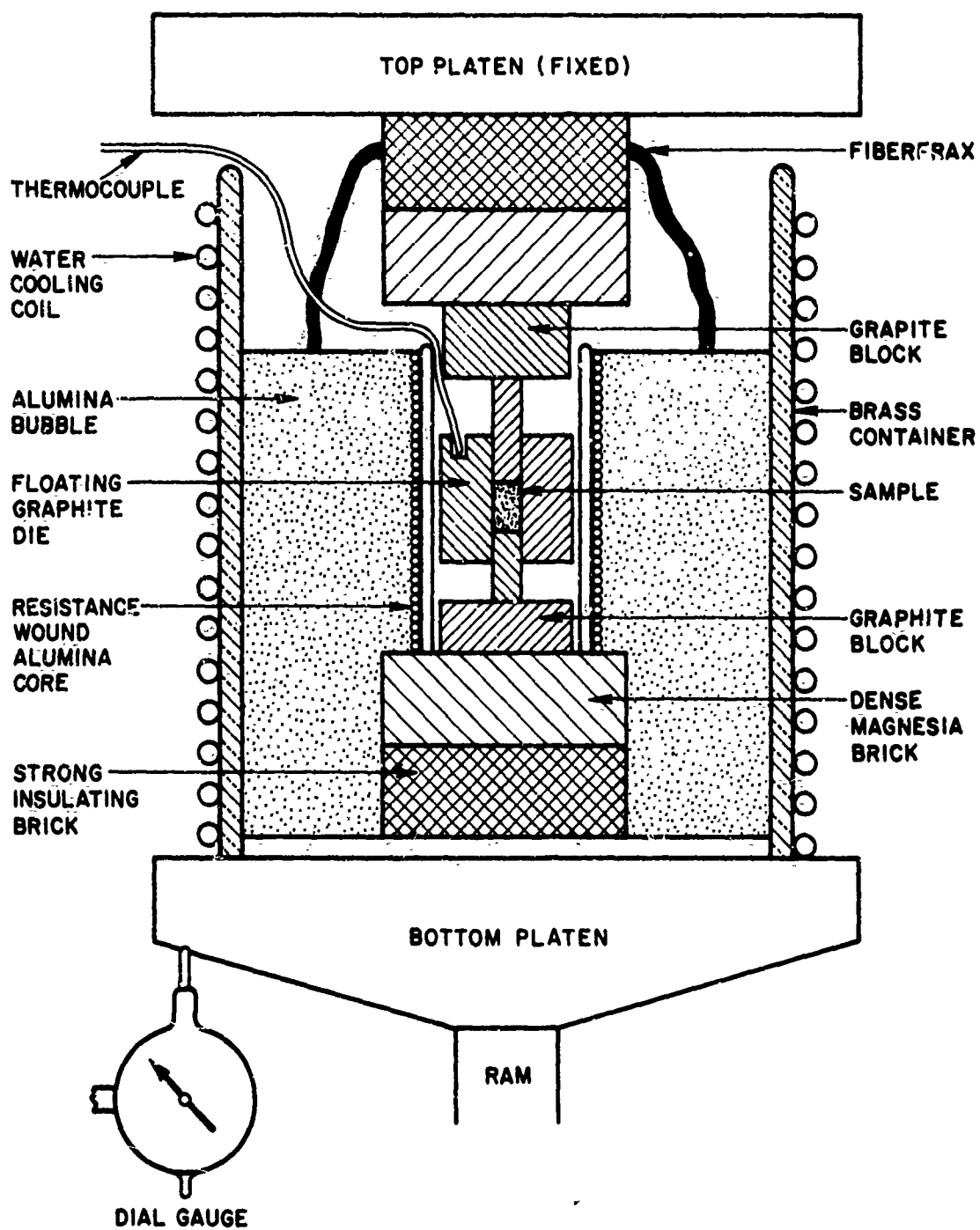


Figure 4. Interior Assembly of Hot Press for Fabrication of 3/4" Diameter Specimens



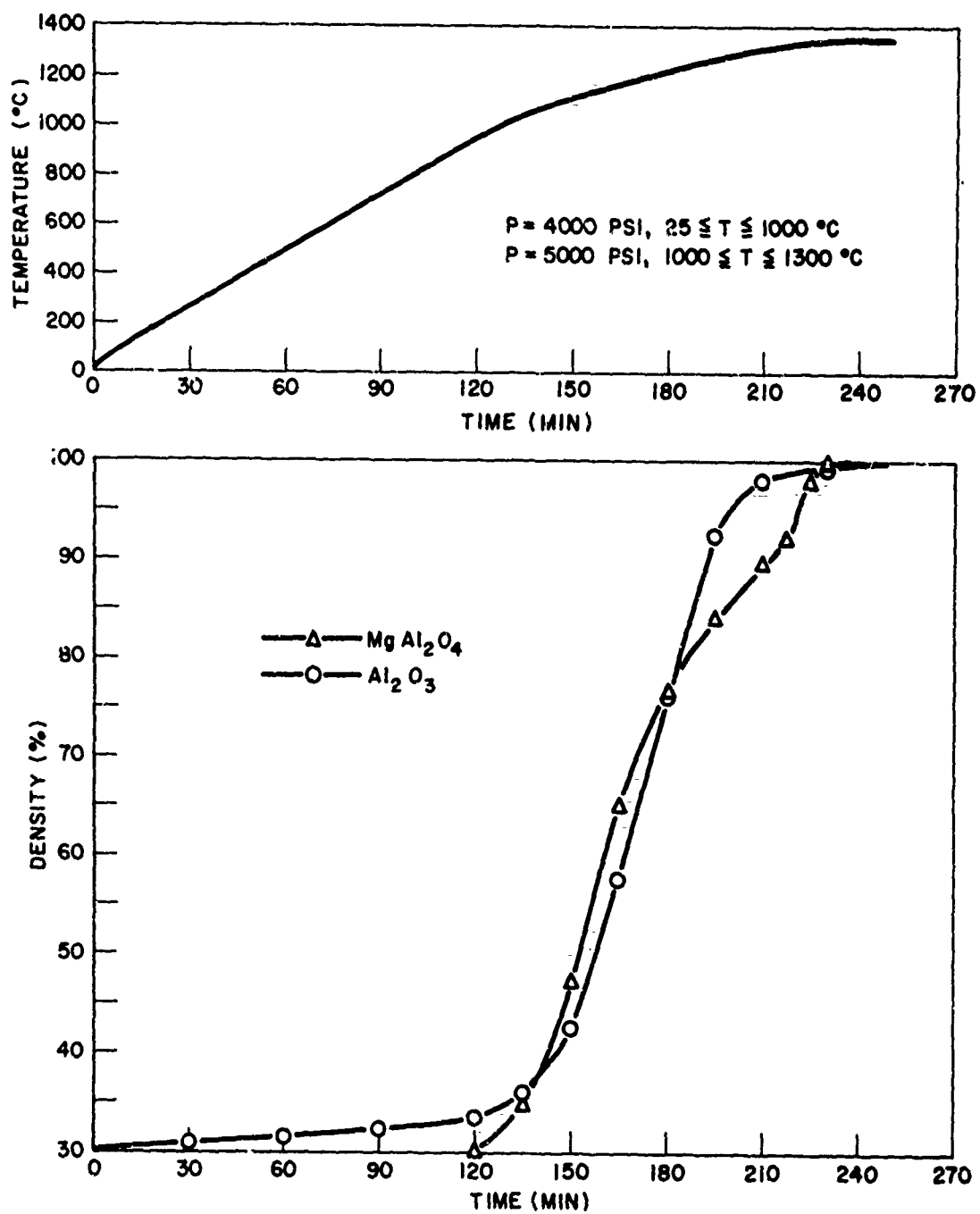


Figure 5. Densification Curves for Pressure Calcintered Alumina and Spinel

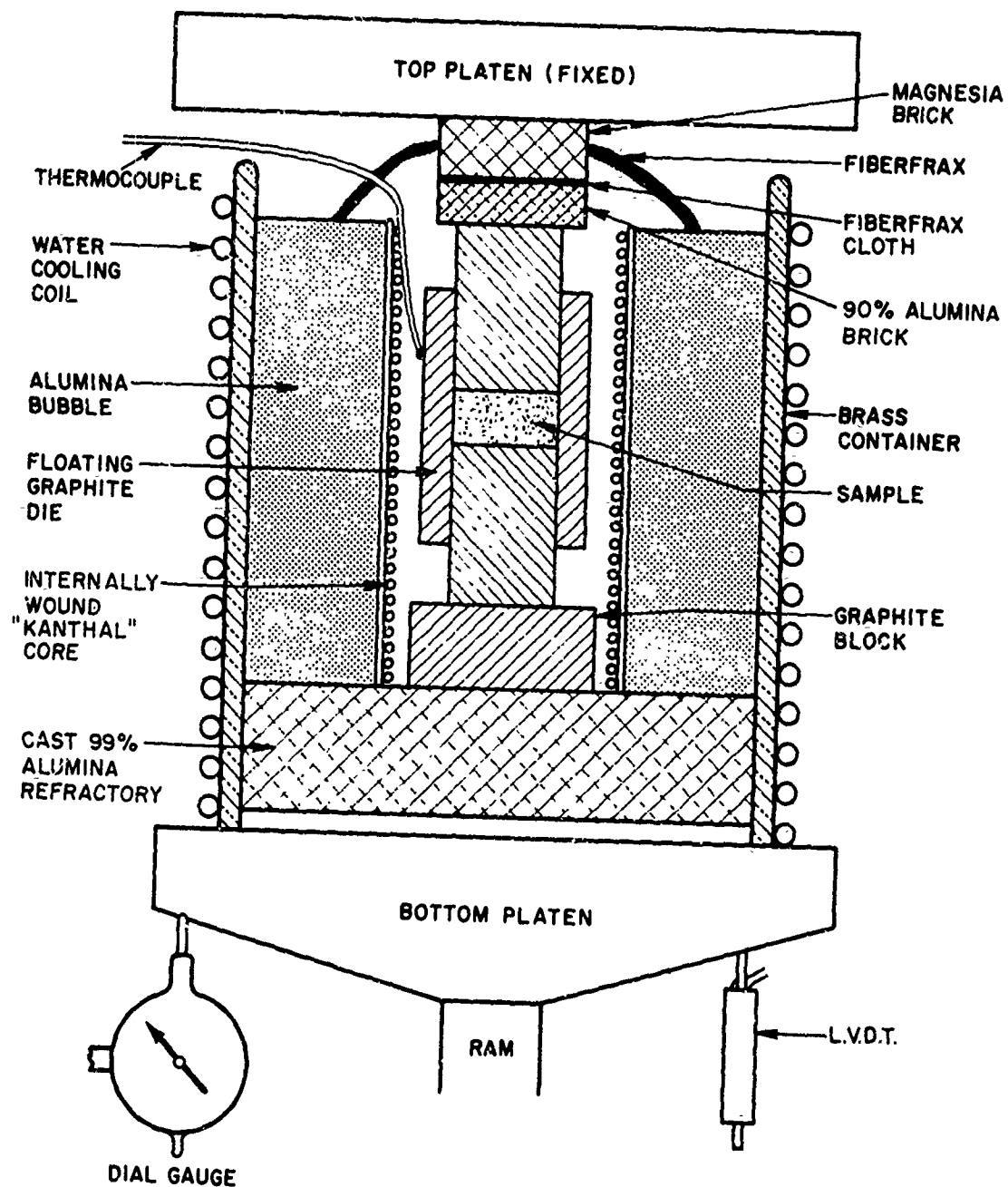


Figure 6. Interior Assembly of Hot Press for Fabrication of 4" Diameter Specimens

The die is heated at 3°C/min to 1350°C, held isothermally at 1350°C for 30 minutes, and then the furnace is turned off. The pressure is decreased to 1000 psi, the hydraulic valves closed off, and the entire hot pressing apparatus is turned off.

Composites with wire mesh or sapphire fibers were fabricated by alternately loading the precursor powder and the reinforcing material into the die and hot pressing as usual. For the production of 4" diameter composite specimens the precursor powder is cold pressed into 4" diameter cylinders at 7000 psi in a steel die. The hot pressing die is then loaded with alternate layers of wire mesh and cold pressed cylinders. The most common composite configuration was a 4" diameter by 3/8" thick specimen containing wire meshes on each end face and one in the center. These composites were formed by loading three wire meshes and two cold pressed cylinders into the hot pressing die.

Sapphire whiskers (0.5μ) were also employed in small reinforced spinel and alumina composites. The whiskers (15 wt. %) were blended with the ceramic precursors in an acetone slurry. The resulting powder was then hot pressed in the usual fashion.

## SECTION IV

### MICROSTRUCTURE

The samples produced by our standard procedures, which were discussed in an earlier section, were typically dense:  $\geq 99\%$  of theoretical density. A list of the pressure calcining runs made during this investigation, including all the densities measured, is given in a previous report.<sup>9</sup>

Following earlier work here, the beneficial effect of Ti ions as a grain growth inhibitor in  $\text{Al}_2\text{O}_3$  was confirmed. Approximately 5 Mole %  $\text{TiO}_2$  in  $\text{Al}_2\text{O}_3$  was found to be the optimum concentration.

Previous work with pressure calcining<sup>3</sup> indicated that this forming method sometimes results in preferred crystallographic orientation in polycrystalline samples. The possibility of preferred orientation in our alumina and spinel samples was investigated by taking X-ray diffraction patterns perpendicular and parallel to the hot pressing direction, and later by standard pole figure techniques. No appreciable evidence of crystallographic texture was found.<sup>9</sup>

The scanning electron microscope was used to characterize the microstructures of the spinel and alumina ceramics and composites. The X-ray fluorescence capability of the microscope was used to great advantage in determining the extent of reaction between reinforcing wires or fibers and the ceramic matrices.

Average grain size was determined from the scanning electron micrographs by simply measuring the image of a typical grain. Fracture surfaces were found to be most reliable for examining grain structures. Quantitative metallographic procedures for measuring grain size were not employed, as they would have been invalid for the nonplanar fracture surfaces. Average grain sizes for both the spinel and alumina ceramics were  $\sim 1\text{-}5\mu\text{m}$ . The grains were typically equiaxed and the grain size distributions were narrow. X-ray fluorescence studies with the scanning electron microscope show that the  $\text{Ti}^{+4}$  dopant in the alumina and spinel matrices is evenly distributed within the grains, confirming the X-ray data that the titania is in solid solution in the matrix materials.

Nichrome mesh reinforced alumina and spinel ceramics were extensively studied by scanning electron microscopy. A typical micrograph of the nichrome-spinel interface is shown in Figure 7. No cracking has been observed at the metal-ceramic interface, even at magnifications up to 10,000X; this was the case for both alumina and spinel.

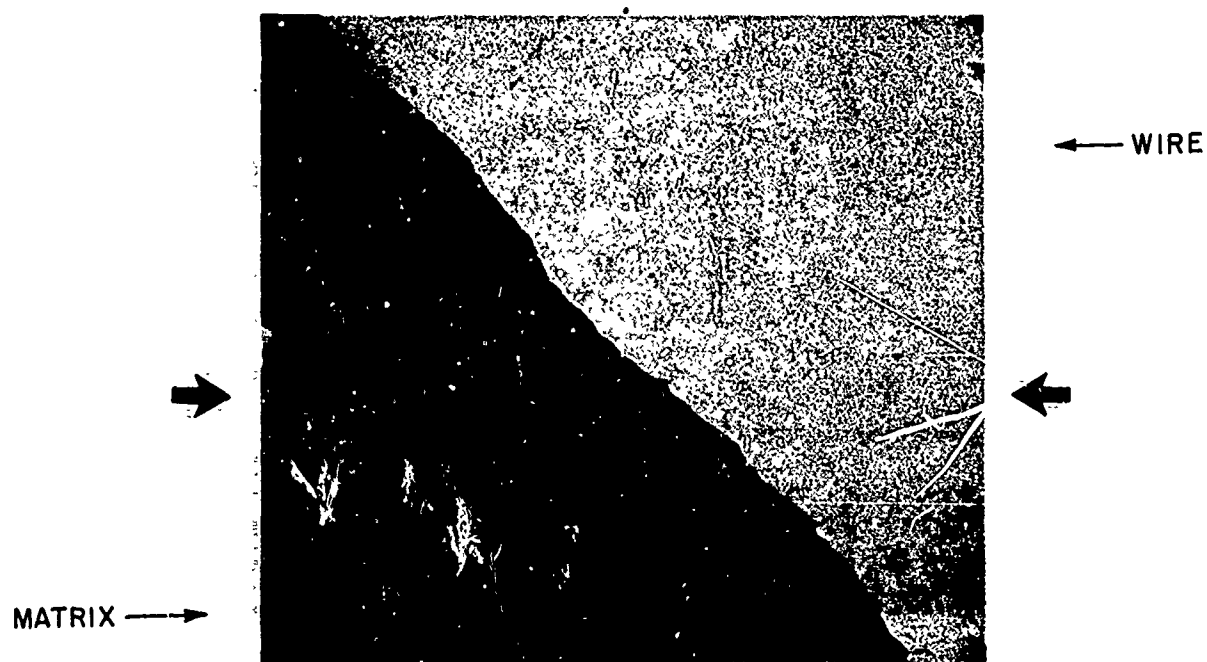


Figure 7. Scanning Electron Micrograph of Spinel-Nichrome Wire Interface. Arrows Indicate Line Scanned for X-ray Fluorescence. X1,000

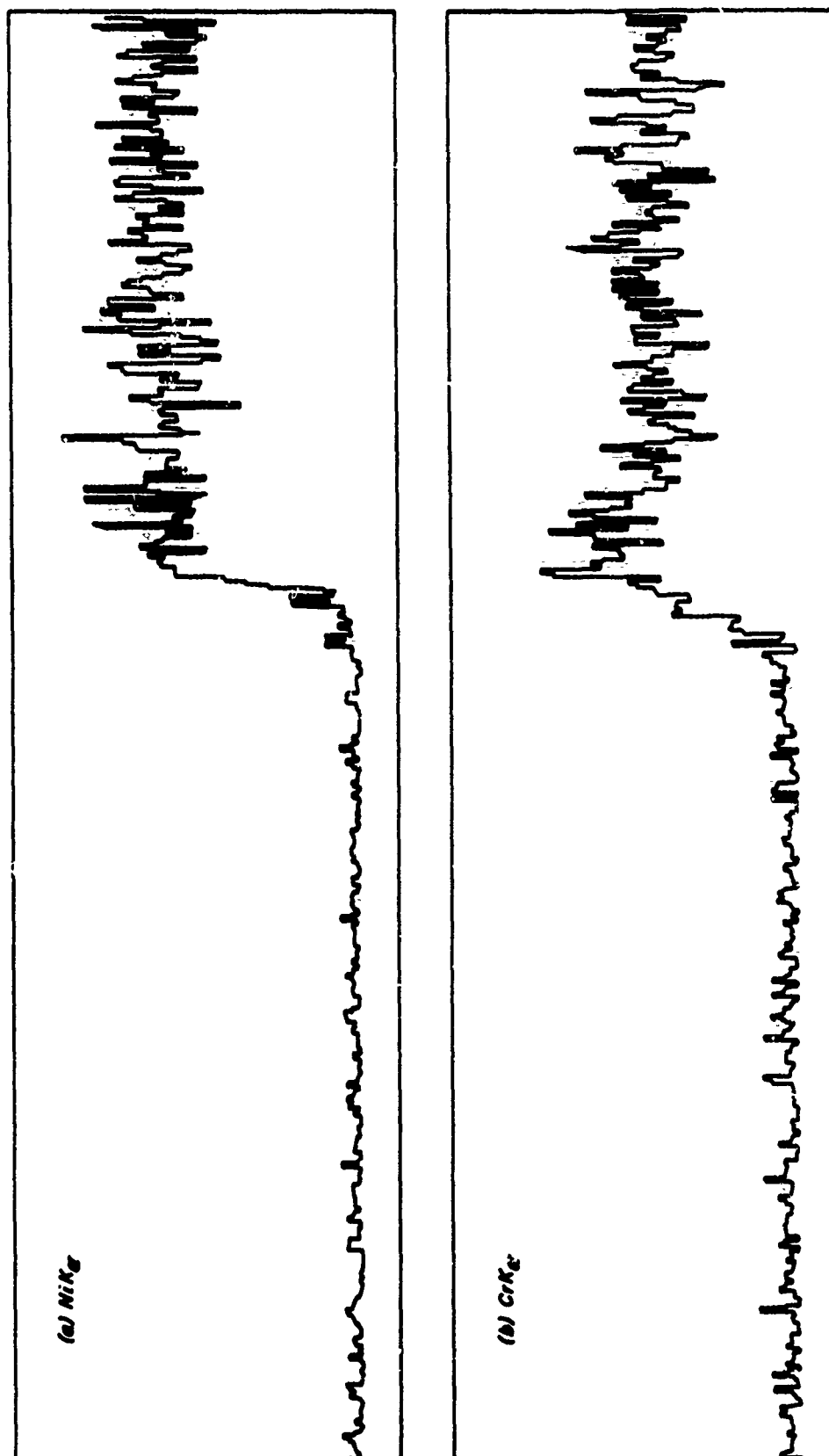


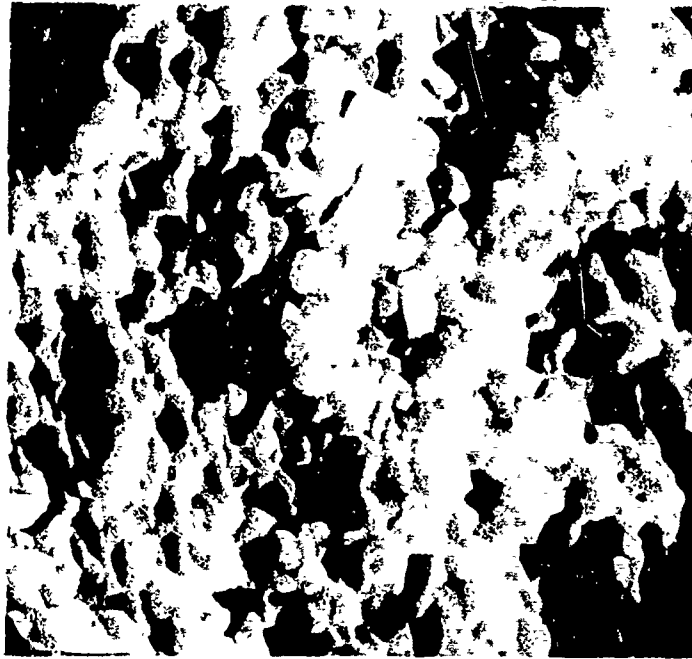
Figure 8. Intensity of Characteristic X-rays Versus Distance  
Across the Nichrome Wire-Spinel Matrix Interface,  
a)  $\text{Ni K}\alpha$ , b)  $\text{Cr K}\alpha$

The thermal expansion coefficients of the metal and ceramics differ by a factor of  $\approx 2$ :  $17 \times 10^{-6}/^{\circ}\text{C}^{10}$  for nichrome,  $8.8 \times 10^{-6}/^{\circ}\text{C}^{11}$  for alumina,  $7.6 \times 10^{-6}/^{\circ}\text{C}^{11}$  for spinel. The higher coefficient of expansion for the nichrome should put the ceramic matrix in compression during cooling, thus strengthening the matrix. This is much more desirable than the reverse case in which the wire or fiber has a lower coefficient of expansion, places the matrix in tension, and often results in microcracks at the interface.<sup>6</sup> The nondispersive X-ray fluorescence capability of the microscope was used to determine the extent of reaction between the nichrome wire and spinel. Figures 8a and 8b are plots of relative concentration (intensity of characteristic X-rays emitted) of Ni and Cr, respectively, versus distance across the sample area scanned. Figure 7 shows the area scanned for these results; a line scan was made across the area indicated by the arrows. The diffusion distances for Ni and Cr into the spinel matrix are  $\approx 5\mu\text{m}$ , i.e., no more than 2-3 spinel grains into the matrix. In alumina Ni diffused  $\approx 5\mu\text{m}$ , Cr  $\approx 40\mu\text{m}$ . Clearly the nichrome wires are not attacked to a significant extent by the matrix materials.

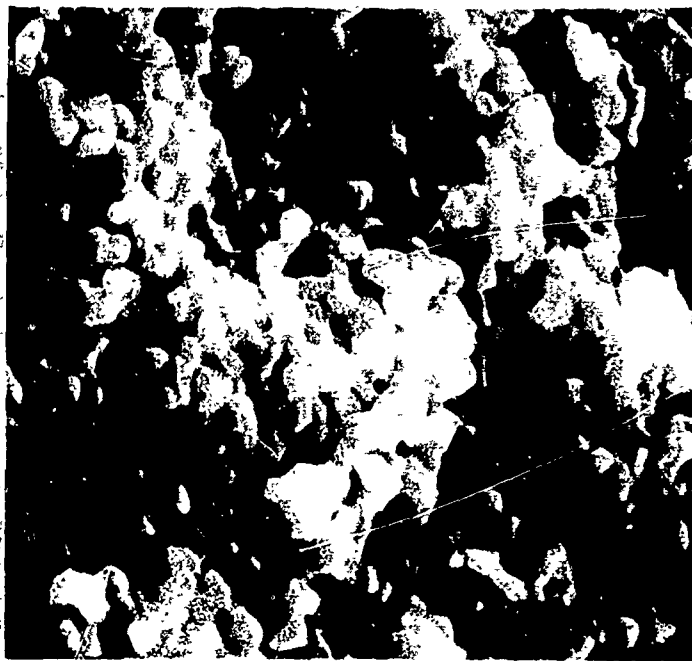
No exaggerated grain growth was observed in the matrix materials near the wire; the grain structure at the interface appeared unaltered relative to the bulk. This is apparent in Figure 9, scanning electron micrographs of wire reinforced alumina.

The nichrome wires remained ductile after fabrication of the composites. Figure 10 shows the ductile failure of nichrome wires in an alumina-nichrome composite. The specimen was fractured as follows: The cylindrical sample was loaded in diametral compression until a single crack was propagated through the matrix across the diameter of the specimen. The sample was then pulled normal to the crack, stretching the exposed wires until they failed. In view of the normal oxidative attack on nichrome at about  $1100^{\circ}\text{C}$ , it appears that oxygen availability is strictly limited under the reactive hot pressing conditions.

Sapphire whiskers could not be found in the microstructures of dense, pressure calcintered spinel and alumina composites fabricated with 15% by weight whiskers. Instead, porous, coarse grained areas were uniformly distributed throughout the material. Figures 11 to 13 illustrate these areas in spinel composites. X-ray fluorescence results from the scanning electron microscope show that these areas are alumina rich. Figure 14 shows the intensity of characteristic Al K $\alpha$  X-rays emitted while scanning across the area shown in Figure 12; the position of the line scan is indicated by arrows. Apparently the whiskers have gone into solution, leaving highly porous, large grained,  $\text{Al}_2\text{O}_3$ -rich areas in the spinel microstructure. The dissolution of sapphire whiskers in oxide materials has been previously observed in conventional hot pressing.<sup>8</sup> The decomposing precursors in a pressure calcintering system are extremely reactive, making dissolution even more likely than in the case of normal hot pressing. The porous, coarse grained areas



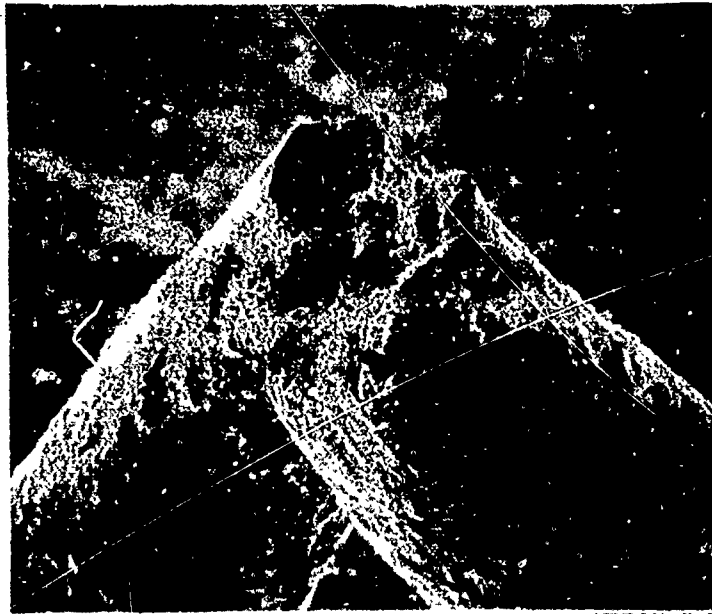
(a)



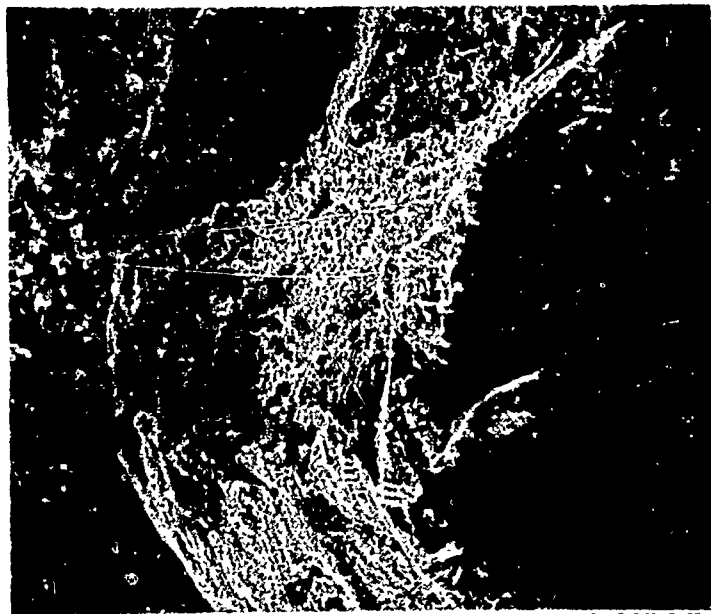
(b)

Figure 9. Scanning Electron Micrograph of Nichrome Wire Reinforced Alumina Showing the Grain Structure (a) Immediately Adjacent to the Wire and (b) Removed from the Wire.  
Fracture Surface X10,000





(a) X100



(b) X300

Figure 10. Scanning Electron Micrograph of Exposed Wire in Fractured Alumina-Nichrome Composite



Figure 11. Macrograph of Pressure Calcintered Spinel Containing 15% by Weight of  $0.5\mu$  Sapphire Whiskers. Fracture Surface, X5.7.

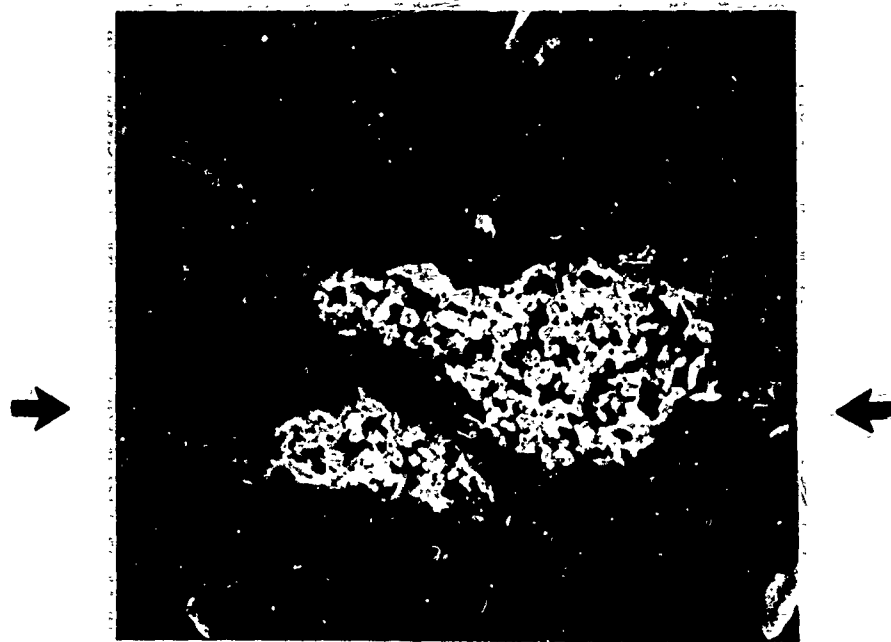


Figure 12. Scanning Electron Micrograph of Pressure Calcintered Spinel Containing 15% by Weight  $0.5\mu$  Sapphire Whiskers. Arrows Indicate Line Scanned for X-ray Fluorescence. X600

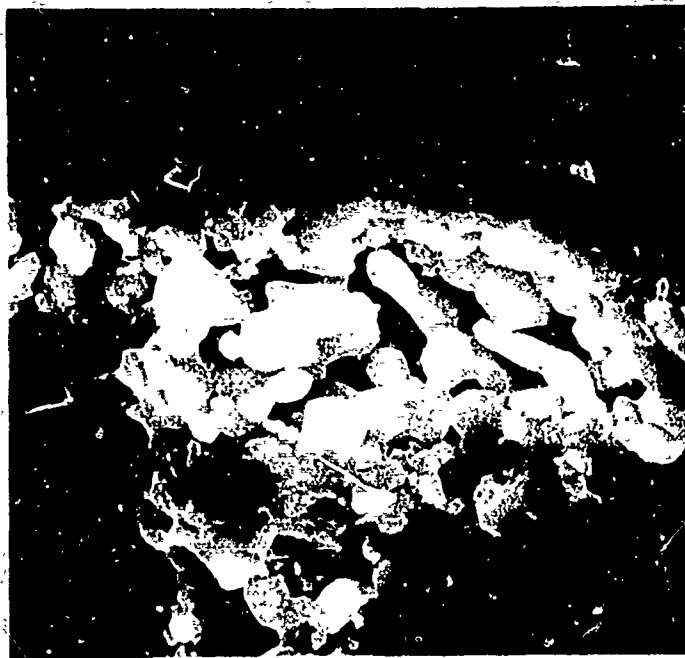


Figure 13. Scanning Electron Micrograph of Pressure Calcintered Spinel Containing 15% by Weight 0.5 $\mu$  Sapphire Whiskers. X3,000.

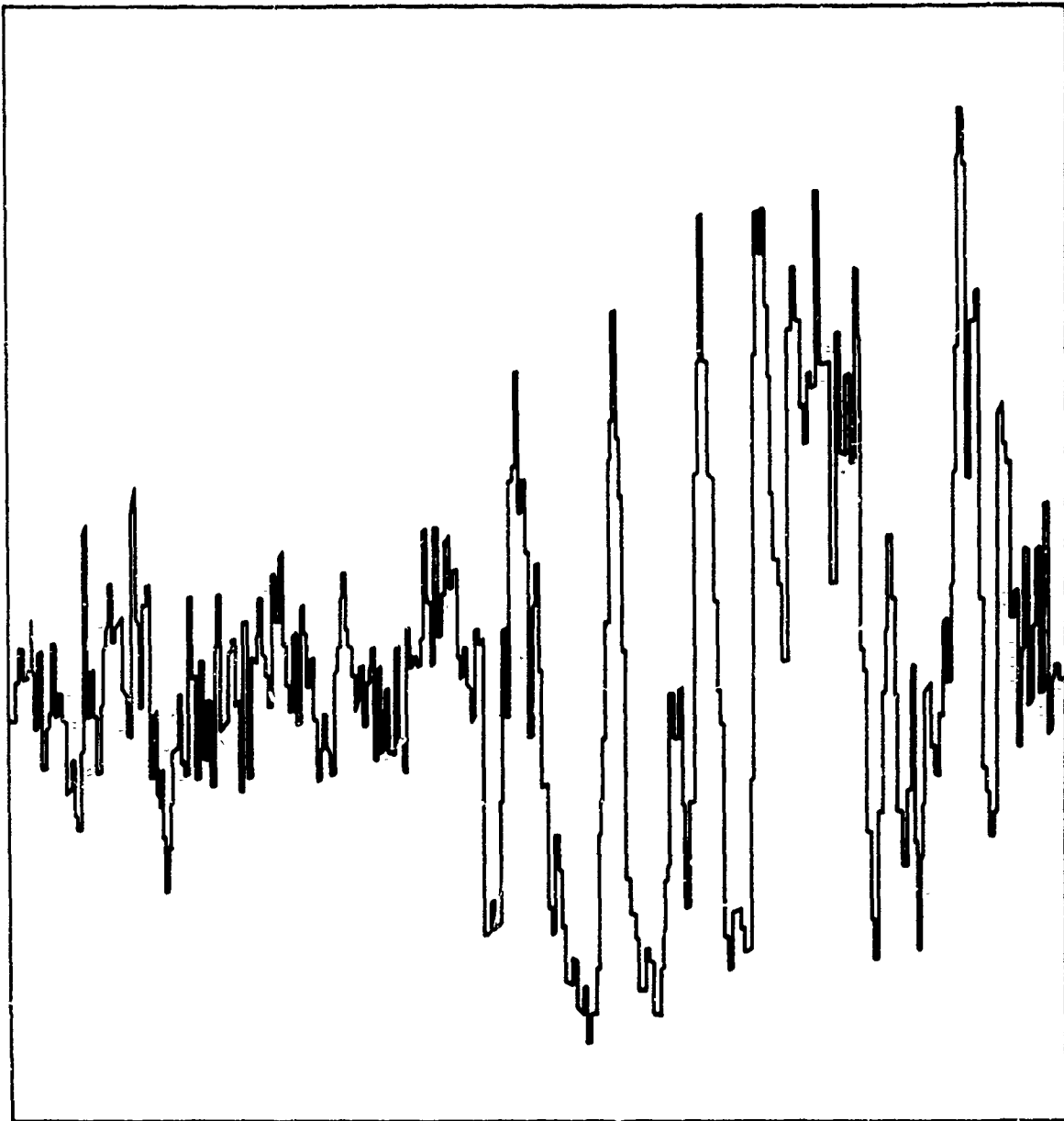


Figure 14. Intensity of Characteristic Al  $K_{\alpha}$  X-rays Versus Distance Across the Sample Area Scanned. Refer to Fig. 12

left behind by the whiskers would seem to be preferred sites for crack initiation. One would not expect these composites to perform well in ballistic tests.

In our early work with composites reinforced with 0.010" sapphire fibers, cylindrical samples 3/4" diameter x 1/2" long were reinforced with four layers of fibers. The fibers within a layer were all parallel; the layers were oriented in a "crisscross" pattern. The fibers in these composites were broken during fabrication. The small broken pieces often recrystallized.<sup>9</sup>

However, it was later found that fragmentation of the sapphire fibers can be avoided if the fibers are well spaced. A fracture surface of a spinel sample containing a single sapphire fiber is shown in Figure 15. The fiber is well bonded to the matrix and remained intact. Multiple cleavage steps are evident on the fracture surface of the sapphire crystal. A glassy looking area  $\approx 7\mu\text{m}$  thick surrounds the sapphire.



(a) X200



(b) X1000

Figure 15. Fractograph of  $\text{MgAl}_2\text{O}_4$  - Sapphire Single Crystal Fiber Composite, Scanning Electron Microscope

## SECTION V

### MECHANICAL PROPERTIES

#### 1. Tensile Strength

Tensile strengths were measured by the diametral compression method. In this test a right circular cylindrical specimen is compressed diametrically between two flat platens. The maximum tensile stresses are developed normal to the loading direction across the loaded diameter. These tensile stresses cause the cylinder to fracture along the diametral plane joining the lines of contact of the specimen and the platens. Since the tensile stresses are directly proportional to the applied load, the tensile strength can be computed from the load at fracture:

$$\sigma_m = \frac{2P}{\pi dt}$$

where

- P = applied load
- d = specimen diameter
- t = specimen thickness
- $\sigma_m$  = maximum tensile stress

Spriggs, *et al*<sup>12</sup> noted that the diametral compression tensile strengths of a large number of ceramic materials were approximately one half the transverse bending strengths.

A sample holder similar to that described by Spriggs, *et al*<sup>12</sup> was used for the diametral compression tests. A schematic diagram of the sample holder is shown in Figure 16. The samples (3/4" diameter x  $\approx$  1/2" long) were tested "as pressed" with no surface treatment other than a rough surface grinding. An Instron testing machine was used to load the samples to failure at a strain rate of 0.002 in./min.

The average diametral compression tensile strengths of the samples tested in this investigation are listed in Table 3. The measured values have been multiplied by 2.0 to make them comparable to frequently cited transverse bending strengths.

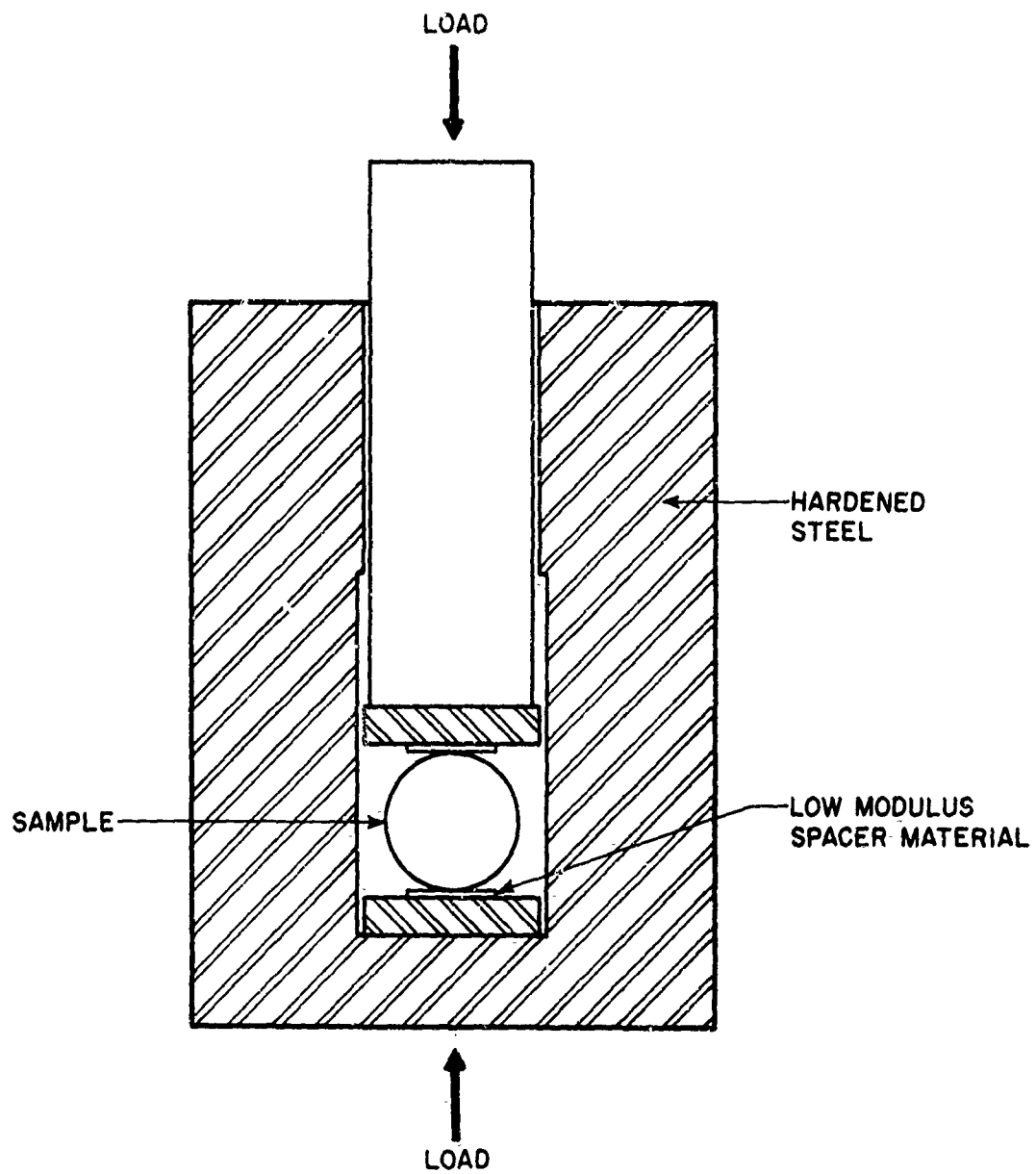


Figure 16. Sample Holder for Diametral Compression Strength Tests



TABLE 3. DIAMETRAL COMPRESSION TENSILE STRENGTHS

<u>Material</u>	<u>Strength, psi</u>
Titania doped alumina	41,512
Titania doped alumina reinforced with four layers of 16x16/in nichrome mesh	21,663
Titania doped alumina reinforced with four layers of 0.010" sapphire fibers	23,038
Titania doped alumina reinforced with 15 weight % sapphire whiskers	34,142
Titania doped spinel	23,161
Titania doped spinel reinforced with four layers of 16x16/in nichrome mesh	11,865
Titania doped spinel reinforced with four layers of 0.010" sapphire whiskers	23,765

Ten samples of titania doped alumina were tested in four-point bending by The Air Force Materials Laboratory. The samples were all cut from a single 3" diameter fully dense hot pressed specimen. The sample dimensions were approximately 2.0" x 0.2" x 0.1". The specimen gage length (inner knife edges) was 0.739"; the outer knife edges were spaced 1.52" apart. The specimens were mechanically ground on silicon carbide grit paper. The testing was done on an Instron testing machine at a crosshead speed of 0.005"/min. The bending strengths are given in Table 4.

**TABLE 4. BEND STRENGTHS OF PRESSURE CALCINTERED ALUMINA**

<u>Specimen</u>	<u><math>\sigma_f</math>, psi</u>
1	51,260
2	39,581
3	39,776
4	67,733
5	50,678
6	53,060
7	40,386
8	45,397
9	38,951
10	<u>47,142</u>
Average	47,397

The ratio of the four-point bending strength to the diametral compression tensile strength for titania doped alumina is  $\approx 2.3$ . Thus the assumption that twice the diametral compression strength = four-point bending strength is a reasonable, if somewhat conservative, estimate.

The strength data for the nichrome mesh-ceramic matrix systems are very interesting in light of the intended ballistic application for these materials. The nichrome reinforced composites fractured at a lower stress than the unreinforced matrix material. However, these composites continued to support an increasing load after the initial fracture. Figure 17 shows representative load-deformation curves for  $Al_2O_3$  and an  $Al_2O_3$  - nichrome composite. The loads are normalized for sample lengths to make the curves for the two samples comparable. The unreinforced  $Al_2O_3$  ceramic failed catastrophically. The nichrome reinforced  $Al_2O_3$  composite showed only the main central crack after initial failure, with the stored elastic energy absorbed, presumably, by plastic deformation of the wire. Figure 18 illustrates the dramatic difference between the types of fracture encountered. If, after the initial diametral crack, loading is continued on the  $Al_2O_3$  - nichrome composite, the sample will continue to support an increasing load with approximately the same load-deformation curve as before fracture. Finally, cracking, of the matrix, delamination, and deformation of the wire occur as the sample gradually crushes.

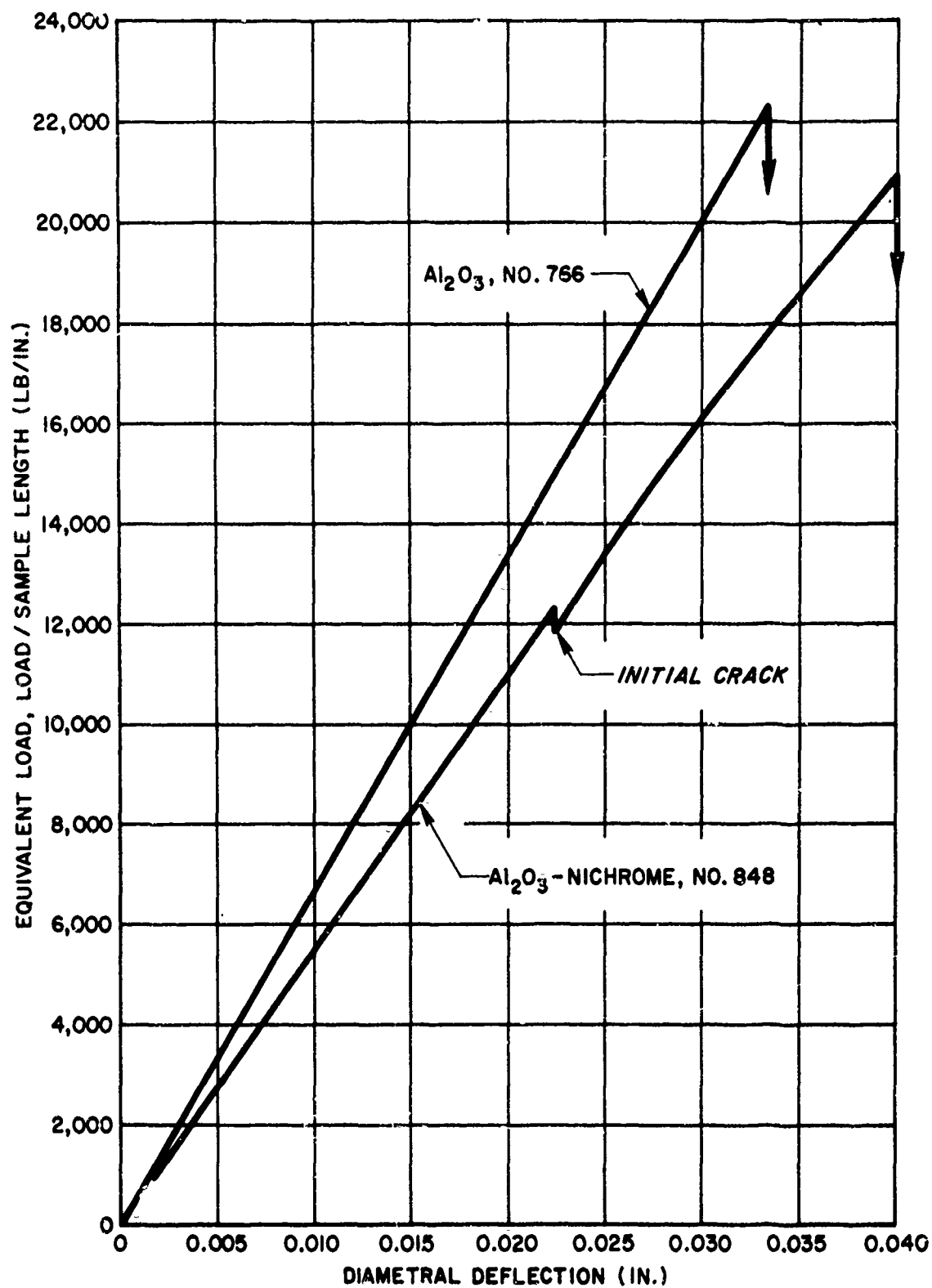


Figure 17. Load-Deformation Curves for Alumina Ceramic and Alumina Nichrome Wire Mesh Composite

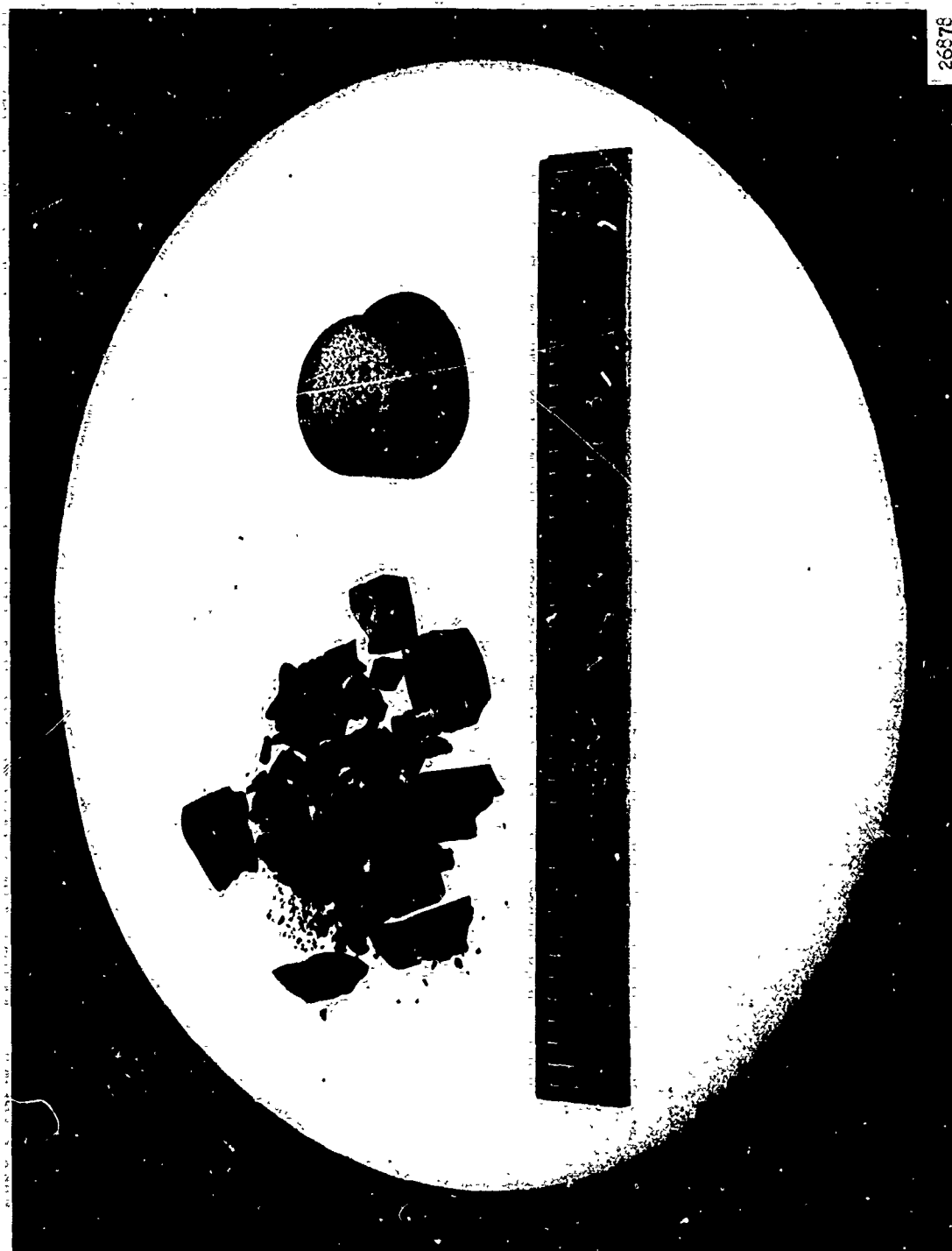


Figure 18. Diametral Compression Test Samples of Alumina (Left) and Nichrome-Alumina Composite (Right) Showing Type of Fracture

The spinel-nichrome samples also continued to support an increasing load after initial fracture. However, some of the spinel-nichrome composites initially failed by delamination.

The strength data for the whisker reinforced composites are not impressive. The whiskers do not reinforce the matrix; they, instead, weaken the material. This is no doubt due to the dissolution of the whiskers during fabrication and the accompanying porous coarse grained areas in the microstructures.

The data for the sapphire fiber reinforced composites is also unimpressive. However, the fibers in these specimens were broken into small pieces during fabrication. To test the effect of unbroken, well bonded sapphire fibers on the strength of spinel, four specimens were fabricated, each containing three parallel fibers lying in a plane parallel to the end faces of the sample. The fibers were not broken during fabrication, and were apparently well bonded to the matrix. Duplicate samples were tested for diametral compression tensile strength as a function of sample orientation to determine the extent of anisotropy in this configuration. The samples were oriented so that the diametral crack ran (1) perpendicularly across the fibers, and (2) in a direction parallel to the fibers. If the sapphire fibers are an effective reinforcement for spinel, we would expect the specimens fractured perpendicularly across the fibers (i.e., through the fibers) to be significantly stronger than those fractured in a direction parallel to the fibers (i.e., between the fibers). The results of those tests are given in Table 5.

TABLE 5. DIAMETRAL COMPRESSION TENSILE STRENGTHS OF SAPPHIRE FIBER REINFORCED SPINEL SPECIMENS

Sample	Density, g/cc	$\sigma$ psi	
		// Fibers	$\perp$ Fibers
1307	3.56	12,766	
1319	3.56	22,844	
1312	3.56		22,982
1336	3.50		21,876

The data in Table 5 indicate that 0.010" sapphire fibers do not significantly strengthen the spinel matrix. Note that none of the specimens is stronger than the average value for unreinforced spinel: 23,161 psi.

## 2. Elastic Modulus

Measurements of sonic modulus were performed on a Sperry Rand UM715 ultrasound reflectoscope, using the reflection method. The transit time resolution for ultrasound pulses on the reflectoscope is  $\approx 1 \mu\text{s}$ . Since the typical transit time of the samples is of the order of several  $\mu\text{s}$ , we have considerably improved the resolution by taking the output from the reflectoscope to a Tektronix oscilloscope. The time scale on the oscilloscope is  $0.01 \mu\text{s}$  enabling the measurement to be made to an accuracy of 1%.

In this method an ultrasound transducer was attached to one face of the cylindrical sample. The faces of the samples had been ground to a smooth finish on a belt sander. The time required for a sound wave to travel through the sample and bounce from the opposite side back to the transducer was read on the time calibrated scale of the oscilloscope. The measurements were usually made at 2.55 or 10 MHz. The thickness of the samples was measured with a micrometer. The velocity of sound travel through the material is obtained from the relation  $2x/t$ , where  $x$  = sample thickness,  $t$  = time.

The longitudinal modulus  $E_L$  is found from the relationship  $E_L = \rho V^2$  where  $V$  is the velocity of ultrasound propagation and  $\rho$  the sample density. Although  $E_L$  is commonly used as an approximation of Young's modulus, the true Young's modulus is a function of both the longitudinal modulus and the shear modulus<sup>13</sup>. The values of  $E_L$  will be systematically higher than the true Young's modulus for alumina and spinel. For example, Schrieber and Anderson<sup>13</sup> measured the longitudinal modulus of Lucalox alumina as  $67.5 \times 10^6$  psi, and the Young's modulus as  $57.8 \times 10^6$  psi.

The modulus of a tungsten sample was measured in order to check the calibration of the apparatus. The tungsten sample had been arc cast and extruded by the manufacturer.\* The material was 100% dense and contained less than 20 ppm carbon and less than 35 ppm oxygen. The measured value for the modulus of tungsten was  $59.8 \times 10^6$  psi, which is in excellent agreement with the literature value,<sup>14</sup>  $59 \times 10^6$  psi.

The longitudinal sonic modulus data from this investigation are listed in Table 6. Additional sonic modulus measurements on titania doped alumina samples have been made by two independent groups at Air Force Materials Laboratory, each yielding good agreement with the data in Table 8. The values are as follows:

Source	Sonic Modulus, $E_L$ , psi
FIRL (Table 8)	$65.8 \times 10^6$
AFML-1, 2 specimens	$69.9 \times 10^6$
AFML-2, 9 specimens	$66.2 \times 10^6$

\*Atlantic Research Corporation, Alexandria, Virginia

TABLE 6. LONGITUDINAL SONIC MODULUS DATA

Material	Sample Number	Thickness cm	Transit Time, $\mu$ sec.	Density, g/cc	Longitudinal Sonic Modulus psi x $10^6$
$Al_2O_3$	774	0.870	1.60	3.95	67.5
"	778	0.890	1.70	3.95	63.3
"	788	0.812	1.55	3.97	63.3
"	828	0.900	1.70	3.94	64.7
"	769	0.814	1.50	3.96	67.4
"	784	0.864	1.75	3.93	56.2
"	576	0.733	1.30	3.96	73.3
"	570	1.222	2.35	3.97	62.6
"	1028	1.030	1.85	3.95	71.0
"	579	0.875	1.60	3.97	<u>69.0</u>
Average					65.8
$Al_2O_3$ - Sapphire Whiskers	853	0.770	1.55	3.79	53.2
"	858	1.548	3.20	3.82	48.4
"	862	1.140	3.00	3.00	<u>25.2</u>
Average					42.4
$MgAl_2O_4$	992	0.839	1.70	3.49	49.6
"	1006	0.500	1.01	3.55	51.7
"	1009	0.576	1.10	3.53	51.5
"	1020	0.572	1.30	3.52	39.7
"	1018	0.326	0.70	3.50	44.0
"	1023	0.620	1.30	3.48	46.0
"	1027	0.581	1.20	3.54	<u>48.3</u>
Average					47.3
$MgAl_2O_4$ - Sapphire Fiber	1151	0.618	1.30	3.55	37.1
"	1164	0.665	1.40	3.55	<u>46.0</u>
Average					41.6

The longitudinal sonic moduli data are difficult to compare with the literature. The longitudinal modulus of our alumina, however, compares favorably with Schrieber's value for Lucalox alumina; a Young's modulus of  $\approx 58 \times 10^6$  psi is indicated.

Ultrasound reflections could not be obtained in the wire mesh reinforced specimens, due to scattering of the sound waves by the wire. Ballistically induced shock waves are believed to interact with the wire mesh in a similar fashion.

The values for sapphire fiber composites reflect only the modulus of the matrix material, as no sonic reflections from the sapphire were observed.

### 3. Microhardness

Microhardness values were determined with a Wilson Tukon microhardness tester, using a Knoop indenter and a 1000g load. The condition of the indenter was checked by making indentations in a standard calibrated test block. The test block had a Knoop hardness of  $755/\text{Kg}/\text{mm}^2$  and had been indented under a 1000g load by the manufacturer. Indentations in the standard test block made by our instrument (1000g load) were virtually identical to the standard indentations.

The filar eyepiece and objective lens in the optical system of the tester were calibrated against a standard magnification scale from an optical microscope. All the measurements in this investigation were made with the same lens; the calibration for that lens is as follows: 1 filar unit =  $0.1633 \mu\text{m}$ .

The samples to be tested were mounted in bakelite and polished on SiC abrasive paper. Once a sample had been indented, Knoop hardness was calculated from the length of the long diagonal of the indentation via the following equation:

$$KHN = L/\ell^2 C_p$$

where



KHN = Knoop hardness number,  $\text{Kg/mm}^2$   
 L = Load applied to indenter, Kg  
 $l$  = Length of long diagonal, mm  
 $C_p$  = Constant for each indenter  
 $C_p$  is supplied along with the indenter by the manufacturer. For the FIRL indenter,  $C_p = 7.028 \times 10^{-2}$

The microhardness data for pressure calcintered alumina and spinel are given in Table 7. Typical optimum values listed by Lynch, *et al*<sup>15</sup> are as follows: 2000-3000  $\text{Kg/mm}^2$  for alumina; 1200  $\text{Kg/mm}^2$  for spinel. The hardness of the FIRL materials differ somewhat from the typical values; the spinel is harder and the alumina softer. Additional research will be required to explain these differences.

The limited microhardness data for nichrome reinforced alumina (Table 8) indicate only moderate degradation of hardness near the wire. The reduced hardness near the wire suggests that wire mesh on the face of a ballistic sample may be undesirable.

TABLE 7. MICROHARDNESS DATA

	Speci- men No.	Average length of Indentations, $\mu\text{m}$	KHN, $\text{Kg/mm}^2$
Titania doped alumina	766	93.0	1645
	774	87.9	1837
	778	83.1	2065
		Average	1849
Titania doped spinel	1023	95.4	1564
	1009	95.8	1551
	1006	93.9	1613
		Average	1576

Table 8. MICROHARDNESS DATA FOR A NICHROME-ALUMINA COMPOSITE

SAMPLE 1034

Distance from wire, m.m.	Length of Indentation, Filar Units	Average Length of Indentation, microns	KHN, Kg/mm <sup>2</sup>
0.2	597 558.5	94.4	1597
0.4	576 588.5	95.1	1577
0.6	603 583.5	95.2	1571
0.8	583 561.5	93.4	1631
1.0	516 500	83.0	2065

#### 4. Fractography of Ballistically Tested Specimens

Standard military ballistic tests were performed on the specimens supplied to Air Force Materials Laboratory by the authors. All the specimens were 4" diameter right circular cylinders. Although specimen size was not investigated, the relatively small size of the test specimens may limit the interpretation of the ballistic results. Representative photographs of the composite materials and configurations tested are shown in Figures 19-29. Figures 19, 26, and 27 are of unreinforced ceramic armor, showing the typical shattering that occurs in these materials. The differences in the fracture modes of the unreinforced ceramics and the wire reinforced composites are apparent.

Figures 20-23 illustrate differences in the fracture behavior of alumina specimens reinforced with 16x16/in and 8x8/in wire mesh. The composites reinforced with the finer 16x16/in mesh had significantly higher ballistic limits than those with the 8x8/in mesh.

The specimens shown in Figures 24 and 25 contain four 16x16/in meshes, and were tested with 50 caliber AP projectiles, as opposed to 30 caliber AP projectiles in all the other tests.

Figures 26-29 are of spinel specimens. The specimens in Figures 26 and 27 are unreinforced, those in Figures 28 and 29 are reinforced with three layers of 16x16/in nichrome mesh. In Figure 27 note that the projectile is embedded in the fiberglass backup plate.

The bonding between the matrix materials and the wire mesh is considered to be very good. Appreciable delamination of the matrix from the wire meshes occurred only within the fracture conoid. Figure 30 shows a fracture surface of a ballistically tested alumina-nichrome composite sample. The specimen is a fractured piece of the test sample shown in Figure 25. The absence of appreciable delamination in the composite is apparent.

A pronounced deformation of the fiberglass backup plate occurred in many of the tests. This deformation was particularly apparent in the 50 caliber tests. Figure 31 shows the backup plate for an alumina specimen reinforced with four layers of 16x16/in mesh and impacted with a 50 caliber AP projectile.

Some of the composite specimens were deformed into a "dish" shape by the ballistic impact. Figure 32 shows the side view of the specimen in Figure 22, and illustrates the deformation of the specimen.

Figures 33 and 34 show the back (exit) side of an alumina specimen reinforced with three layers of 16x16/in nichrome mesh - one mesh on each face and one in the center. Note the direction in which the wires are bent: The wires on the front face point frontwards, opposite to the direction of motion of the bullet, while the middle and back layers of wire point backwards, in the same direction as the projectile. The wire meshes were bent into conical shapes by the ballistic impact.

The composite specimens reinforced with 16x16/in wire meshes show only a relative few radial cracks, and almost no concentric cracks. (See Figures 20,24,25,28,29,30,33,34.) Many of the composites containing the larger 8x8/in mesh have very interesting, and yet unexplained fracture patterns. Radial cracks frequently branch out into three or more cracks; concentric cracks are visible, and radial cracks are initiated at concentric cracks. Figures 35 and 36 illustrate these fracture patterns.

The ballistic limit, normalized for areal density, of alumina and spinel ceramics is decreased by the addition of wire mesh in the composite configurations tested. Clearly the fracture mode is altered by the addition of wire mesh, and a second hit capability is attained. Significant differences in the ballistic limit of composites having different wire mesh sizes, 8x8/in or 16x16/in, were found; the smaller mesh composites gave greater protection.



Figure 19. Ballistically Tested Alumina Specimen

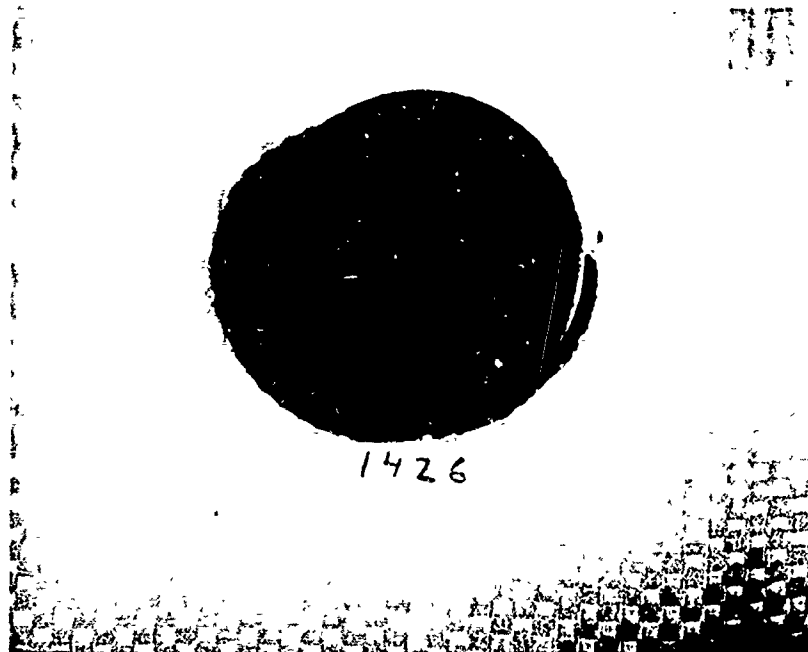


Figure 20. Ballistically Tested Alumina-Nichrome Wire Mesh Composite, 3 16x16/in Wire Meshes



Figure 21. Ballistically Tested Alumina-Nichrome Wire Mesh Composite, 3 8x8/in Meshes

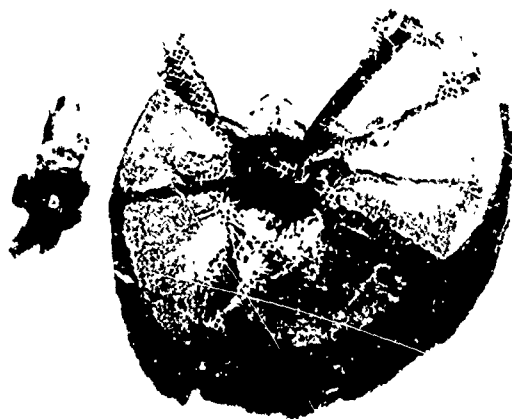


Figure 24. Ballistically Tested Alumina-Nichrome Wire Mesh Composite, 4 16x16/in Meshes, 50 Caliber Shot



Figure 25. Ballistically Tested Alumina-Nichrome Wire Mesh Composite, 4 16x16/in Meshes, 50 Caliber Shot

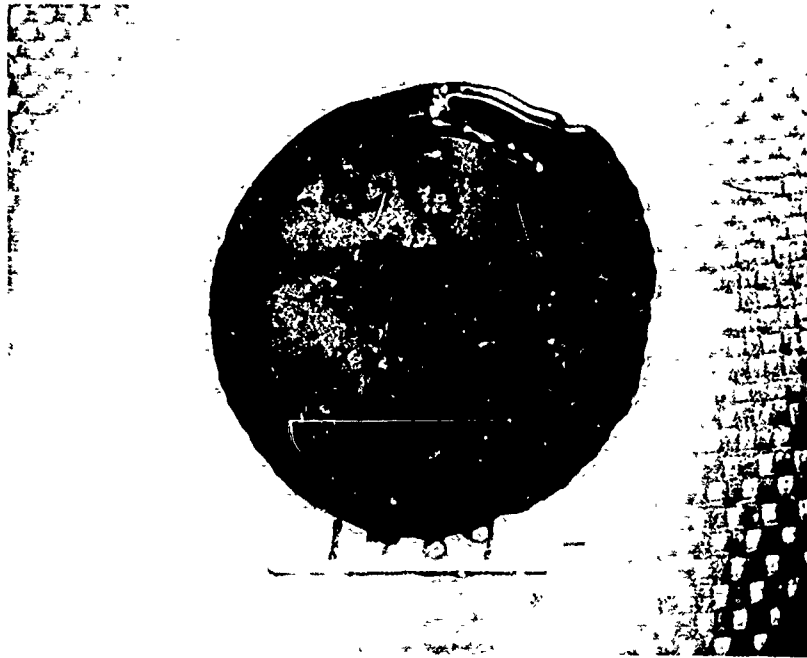
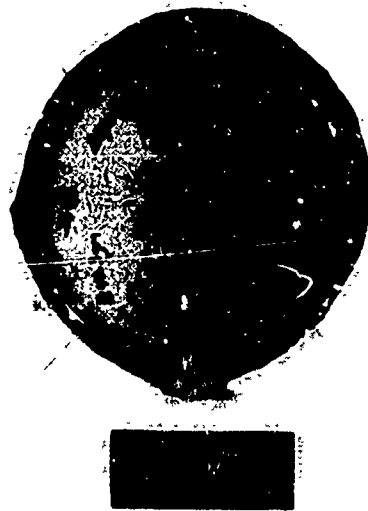


Figure 28. Ballistically Tested Spinel-Nichrome Wire Mesh Composite, 3 16x16/in Meshes



*SHOT #*

Figure 29. Ballistically Tested Spinel-Nichrome Wire Mesh Composite, 3 16x16/in Meshes



TABLE 3. DIAMETRAL COMPRESSION TENSILE STRENGTHS

<u>Material</u>	<u>Strength, psi</u>
Titania doped alumina	41,512
Titania doped alumina reinforced with four layers of 16x16/in nichrome mesh	21,663
Titania doped alumina reinforced with four layers of 0.010" sapphire fibers	23,038
Titania doped alumina reinforced with 15 weight % sapphire whiskers	34,142
Titania doped spinel	23,161
Titania doped spinel reinforced with four layers of 16x16/in nichrome mesh	11,865
Titania doped spinel reinforced with four layers of 0.010" sapphire whiskers	23,765

Ten samples of titania doped alumina were tested in four-point bending by The Air Force Materials Laboratory. The samples were all cut from a single 3" diameter fully dense hot pressed specimen. The sample dimensions were approximately 2.0" x 0.2" x 0.1". The specimen gage length (inner knife edges) was 0.739"; the outer knife edges were spaced 1.52" apart. The specimens were mechanically ground on silicon carbide grit paper. The testing was done on an Instron testing machine at a crosshead speed of 0.005"/min. The bending strengths are given in Table 4.



Figure 30. Fracture Surface of Ballistically Tested Alumina-Nichrome Composite

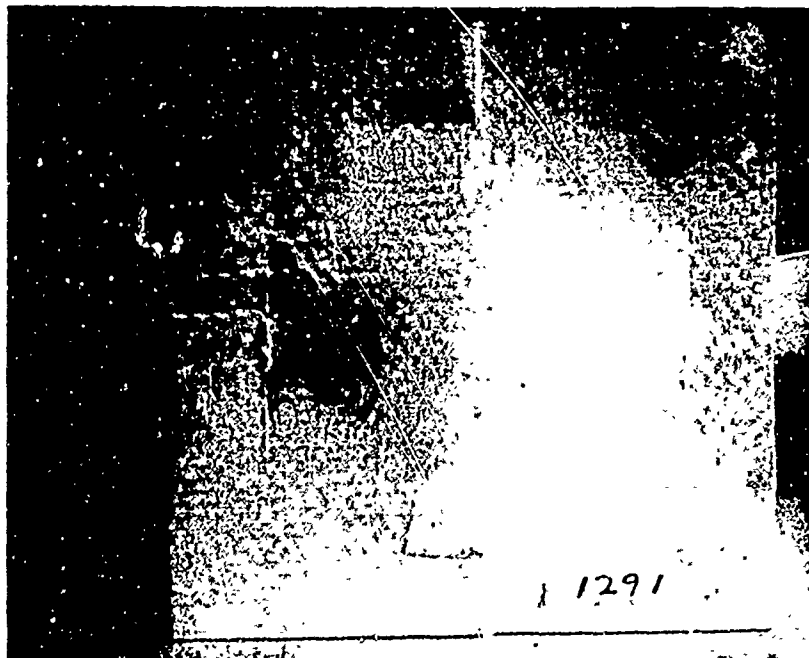


Figure 31. Backup Plate after Ballistic Test of Alumina-Nichrome Composite



Figure 32. Side View of Ballistically Tested  
Alumina-Nichrome Composite

Ballistic Impact was on the Bottom Side  
of the Specimen



Figure 33. Back (Exit) Side of Ballistically Tested Alumina-Nichrome Composite

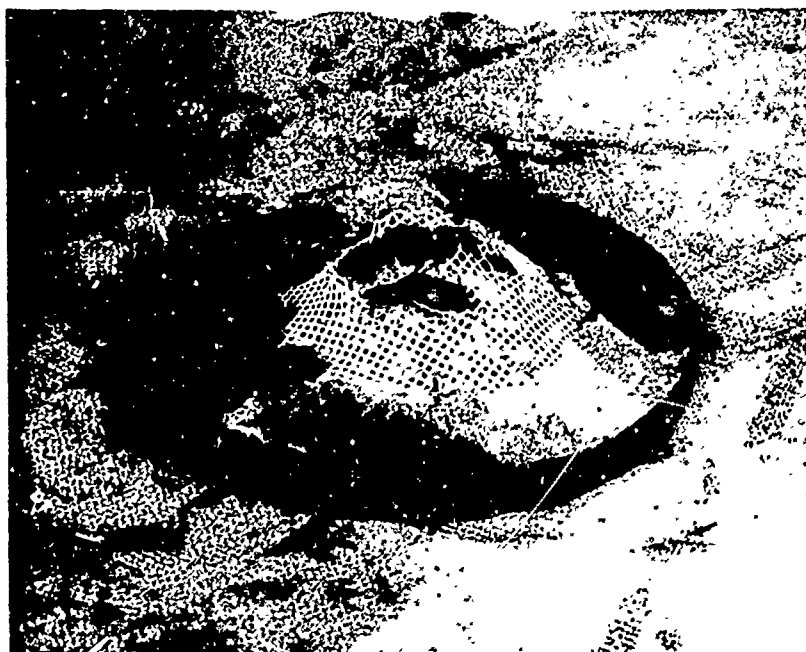


Figure 34. Back (Exit) Side of Ballistically Tested Alumina-Nichrome Composite

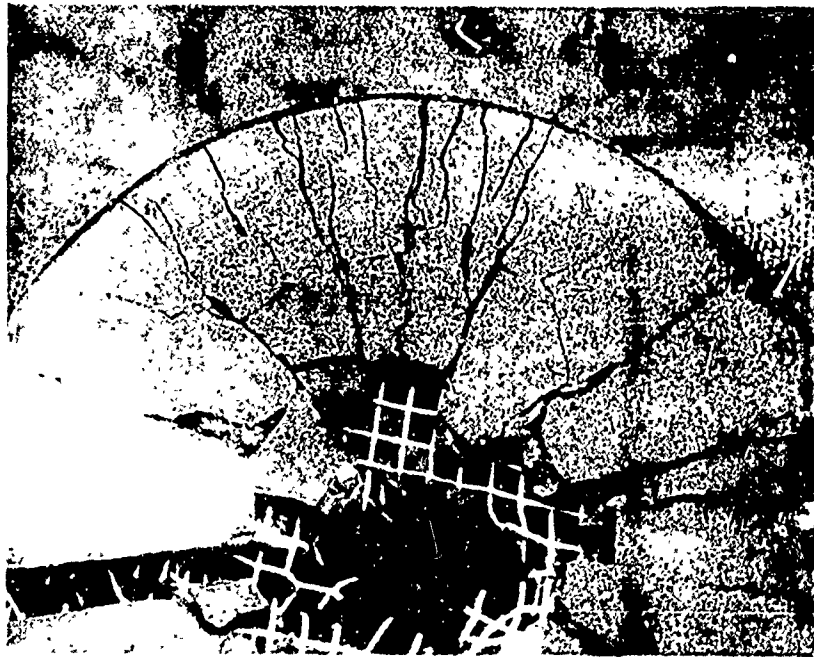


Figure 35. Ballistically Tested Alumina-Nichrome Composite

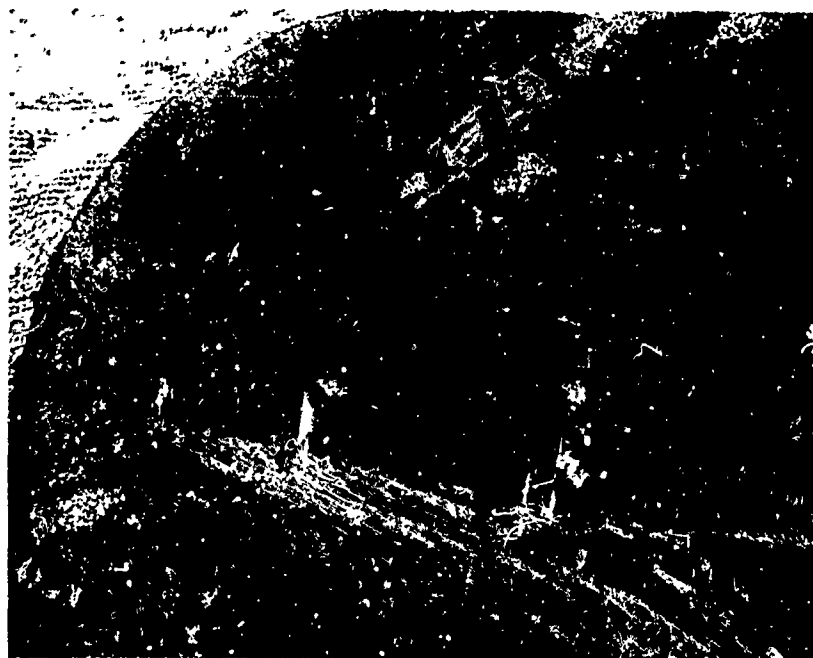


Figure 36. Ballistically Tested Alumina-Nichrome Composite

## SECTION VI

### CONCLUSIONS

1. Titania doped  $\text{Al}_2\text{O}_3$  and  $\text{MgAl}_2\text{O}_4$  ceramics can be fabricated into fully dense, fine grained (1-5 $\mu\text{m}$ ) polycrystalline shapes at moderate temperature, 1350°C, and pressure, 4000-5000 psi, by the method of pressure calcinering. Specimens as large as 4" diameter x 3/4" thick right circular cylinders have been fabricated.

2. Nichrome wire mesh can be incorporated into pressure calcin-tered  $\text{Al}_2\text{O}_3$  and  $\text{MgAl}_2\text{O}_4$  matrices to form dense composites with little or no degradation of either the wire mesh or the ceramic matrix.

3. The incorporation of sapphire whiskers and fibers into spinel and alumina matrices did not significantly improve the room temperature mechanical properties of the matrix materials.

4. Although the ballistic limit, normalized for areal density, of alumina and spinel ceramics is decreased by the addition of wire mesh in the composite configurations tested, the fracture mode is significantly altered by the addition of wire mesh. A second hit capability is attained which may be of importance.

5. Significant differences in the ballistic limit of composites having different wire mesh sizes, 8x8/in or 16x16/in, were found; the smaller mesh composites gave greater protection.

## SECTION VII

### RECOMMENDATIONS FOR FUTURE WORK

The present work shows conclusively that metal wires can be well bonded into dense, fine grained ceramic matrices. Preliminary, unpublished work by the authors indicates that metal powders can likewise be incorporated into dense coherent, mechanically sound ceramics by pressure calcintering.

Clearly, the presence of metal wires influences crack initiation and crack propagation in these composites, but the mechanisms of failure are not fully understood. For example, the present work indicates that wire mesh size is a significant variable in wire mesh-ceramic composites, but no criterion for choosing optimum wire mesh sizes, wire diameters, or spacing of meshes is at hand.

Nichrome was chosen for this work because of its oxidation resistance, thus facilitating low temperature fabrication in air. But how does one choose the best metal to reinforce a given ceramic matrix, strength/weight ratio, coefficient of thermal expansion, bonding ability, etc.? If metal reinforcement interacts with shock wave propagation through the composite, then density and elastic modulus of the metal, relative to that of the ceramic, and spacing of the metal constituents may be the important variables for ballistic armor composites.

Metal-ceramic composites of the type developed in the present work may have interesting applications as high temperature structural members, in which case the oxidation resistance of the composites will be important. Graded metal-ceramic composites may be useful in structural applications where ceramic to metal seals are necessary or desirable. Thermal expansion of these composites will obviously be important.

A systematic theoretical and experimental study on model systems is obviously needed in order to develop adequate guidelines for design of metal-ceramic composites for ballistic and other structural applications. The system alumina-nichrome is recommended for the study of configurational parameters, because of the relative ease of fabrication and the data already generated in the present work.

## REFERENCES

1. P. E. D. Morgan and E. Scala, *The Formation of Fully Dense Oxides by the Decomposition Pressure Sintering of Hydroxides*, presented at the 67th Annual Meeting, Am. Ceram. Soc., Phila., Pa., May 3, 1965.
2. P. E. D. Morgan and N. C. Schaeffer, *Chemically Activated Pressure Sintering of Oxides*, Progress Report No. 4., Contract No. AF33(615)-3065, December 1965.
3. P. E. D. Morgan and N. C. Schaeffer, *Chemically Activated Pressure Sintering of Oxides*, Report AFML-TR-66-356, Part I, November 1966.
4. P. E. D. Morgan and E. Scala, *High Density Oxides by Decomposition Pressure Sintering of Hydroxides*, Proc. Intl. Conf. on Sintering and Related Phenomena, Notre Dame, Inc., June 1965, Publ. 1967, Gordon and Breach, Ed. G. C. Kuczynski.
5. E. Scala, N. C. Schaeffer, R. Penty, *Chemically Activated Pressure Sintering of Oxides for Composites*, Progress Report No. 5 under Contract No. AF33(615)-3065, Materials Science and Engineering, Cornell University, Ithaca, New York (issued March 27, 1967).
6. E. Scala, N. C. Schaeffer and R. A. Penty, *Chemically Activated Pressure Sintering of Oxides*, Technical Report No. AFML-TR-66-356, Part II, May 1968.
7. A. M. Alper, et al, *The System MgO-MgAl<sub>2</sub>O<sub>4</sub>*, J. Am. Cer. Soc., 45 [6] 263-268, 1962.
8. W. R. De Boskey and H. Hahn, *Opaque Lightweight Armor*, Final Report, Contract No. N178-9003, U. S. Naval Weapons Laboratory.
9. D. R. Johnson and P. E. D. Morgan, *Ceramic Matrix Composites as Armor Materials*, Technical Report AFML-TR-70-54, Part I, Air Force Materials Laboratory, Wright-Patterson Air Force Base, Ohio, April 1970.
10. Taylor Lyman, Ed., *Metals Handbook*, Vol. 1, eighth edition, Metals Park, Ohio: Am. Soc. Metals, 1961.
11. W. D. Kingery, *Introduction to Ceramics*, John Wiley and Sons, 1960.
12. R. M. Spriggs, et al, *Tensile Strength of Dense Polycrystalline Ceramics by the Diametral-Compression Test*, Materials Research and Standards, May 1964, pp. 218-220.



13. E. Schrieber and O. L. Anderson, "*Pressure Derivatives of the Sound Velocities of Polycrystalline Alumina*," J. Am. Ceram. Soc. 49(4) 184-190 (1966).
14. Peter T. B. Shaffer, *High Temperature Materials*, No. 1, Material Index, N. Y.: Plenum Press, 1964.
15. J. F. Lynch, et al, "*Engineering Properties of Ceramics*," Tech. Rept. AFML-TR-66-52, June 1966.